frontiers in Materials

ORIGINAL RESEARCH
published: 18 February 2021
doi: 10.3389/fmats.2021.583112

Experimental Study on an Innovative Biopolymeric Treatment Against Salt Deterioration of Materials in Cultural Heritage

Mattia Bassi[1], *Enrico Sassoni*[1,2] *and Elisa Franzoni*[1,2]*

[1]Interdepartmental Centre for Industrial Research in Building and Construction (CIRI Building and Construction), University of Bologna, Bologna, Italy, [2]Department of Civil, Chemical, Environmental and Materials Engineering (DICAM), University of Bologna, Bologna, Italy

Salt crystallization is one of the harshest deterioration mechanisms affecting heritage materials, causing impressive decay patterns and the loss of a high thickness of original materials. Although salt damage has been widely investigated in the literature from the theoretical and experimental points of view, the solutions to mitigate this problem are still extremely limited. In the present paper, a new biopolymeric treatment based on chitosan was tested on two kinds of porous limestones widely used in historic architecture, aiming at inhibiting the crystallization of sodium sulphate inside the stone and promoting the formation of salt efflorescence over the surface, rather than harmful subflorescence inside the pore network. The treatment was applied to the bare stone and also after an inorganic pre-treatment based on the formation of hydroxyapatite in the stone. Hydroxyapatite was recently proposed for the consolidation and protection of carbonate stones and here it is expected to provide an effective anchoring layer for the chitosan coating on the pores surface, and also to prevent the calcite washout from the stone and hence the removal of chitosan. The effect of hydroxyapatite alone was also tested, for comparison's sake. Treated and untreated stone specimens were subjected to two different accelerated salt crystallization tests, one based on crystallization cycles (wetting-drying cycles) and the other one based on continuous capillary absorption of a saline solution ("wick effect"), evaluating the results in terms of weight loss, efflorescence formation, and changes in porosity and mechanical properties. The results showed that all the treatments are compatible with the stones, and the combined treatment (hydroxyapatite + chitosan) is extremely promising for the prevention of salt damage.

Keywords: chitosan, hydroxyapatite, salt inhibitor, sodium sulphate (mirabilite and thenardite), biopolymer, efflorescence, limestone, salt crystallization tests

OPEN ACCESS

Edited by:
Guang-Ling Song,
Xiamen University, China

Reviewed by:
Dusan Losic,
University of Adelaide, Australia
Peng Wang,
Harbin Medical University, China
Pagona-Noni Maravelaki,
Technical University of Crete, Greece

***Correspondence:**
Elisa Franzoni
elisa.franzoni@unibo.it

Specialty section:
This article was submitted to Environmental Materials, a section of the journal Frontiers in Materials

Received: *15 July 2020*
Accepted: *08 January 2021*
Published: *18 February 2021*

Citation:
Bassi M, Sassoni E and Franzoni E (2021) Experimental Study on an Innovative Biopolymeric Treatment Against Salt Deterioration of Materials in Cultural Heritage. Front. Mater. 8:583112. doi: 10.3389/fmats.2021.583112

INTRODUCTION

One of the major causes of deterioration and damage of cultural heritage is the presence of salts within historic building materials such as stone, brick, mortars and plasters, and also in more recent materials such as concrete (Charola, 2000; Sandrolini and Franzoni, 2007; Doehne and Price, 2010; Espinosa-Marzal and Scherer, 2010; Franzoni, 2014; Charola and Bläuer, 2015; Charola and Wendler, 2015; Lubelli et al., 2018; Andreotti et al., 2019). Damage is caused by crystallization

of salts, due to evaporation and/or cooling of saline solutions, and in particular by the solubilization/crystallization cycles, due to the strong sensitivity of salts to the thermo-hygrometric conditions. This leads to formation of internal mechanical stress in the material, protracted over time. In most cases, this stress can easily overcome the tensile strength of building materials, usually quite low, causing formation and propagation of cracks, which affect structural and decorative elements of buildings (Flatt, 2002; Scherer, 2004).

Salts can enter building materials in different ways, the main one being certainly the capillary absorption of moisture from the soil (Charola, 2000; Doehne and Price, 2010; Franzoni, 2014; Charola and Bläuer, 2015; Charola and Wendler, 2015). In this case, water coming from rain, underground water sources or broken pipes, filters through the ground dissolving the salts contained in it. The saline solution is absorbed by the wall by capillarity, up to a height that depends on the evaporation rate, related to thermo-hygrometric conditions (temperature, T, and relative humidity, RH) and materials porosity (Sandrolini and Franzoni, 2007; Charola and Bläuer, 2015; Charola and Wendler, 2015). As long as the water supply is greater than the evaporation rate, the wall will appear wet on the surface and salts will crystallize over the surface as efflorescence, involving mainly aesthetical damage. When the evaporation rate increases, the evaporation front will move inwards, where the salt solution will reach the supersaturation necessary for the crystallization of salts within the porous network of the materials, causing formation of potentially harmful subflorescence (Franzoni, 2014; Andreotti et al., 2019). In addition to capillary rise, salts can be autochthonous in the materials (for example, in Portland cement or in bricks) or can come from external sources such as deicing salts used in roads, from chemical products used in agriculture, from marine spray in the case of buildings near the coast or from the chemical reactions between building materials and air pollutants (Charola and Bläuer, 2015; Charola and Wendler, 2015).

Over the last decades, the phenomenon of damage caused by salt crystallization has been widely studied and many theories have been formulated. It is now clear that, following evaporation or cooling of a salt solution, supersaturation conditions are reached, i.e., conditions where the concentration of salt dissolved in solution is greater than the saturation one, at the same temperature: in this case, salt crystals precipitate in the pores of the material (Scherer, 2004; Doehne and Price, 2010). As a crystal grows and approaches the inner pore wall, repulsive forces arise to prevent the direct contact between the two surfaces: this "disjoining pressure" is attributed to repulsive Van der Waals forces in the case of ice or to electrostatic forces in the case of salt crystals (Scherer, 1999; Houck and Scherer, 2006; Andreotti et al., 2019). Therefore, the two surfaces organize the orientation of the water molecules and ions in different ways, to minimize their surface energy, and this prevents the direct contact between the crystal and the pore wall, allowing the persistence of a thin liquid film (a few nanometers thick) (Scherer, 1999). Internal tensile forces are generated in this liquid film and, if this layer did not exist, the crystal would not damage the material. However, the energy necessary to overcome repulsive forces (energy that would allow direct contact between the surfaces) is usually greater than the tensile strength of the material and this causes the formation of cracks and the subsequent failure of the material itself (Houck and Scherer, 2006; Espinosa-Marzal and Scherer, 2010). The amount of damage will depend on various factors, first of all the degree of supersaturation reached, which in turn is influenced by the type of salt, material porosity, pore size distribution, etc. (Scherer, 2004; Angeli et al., 2007).

Increasing the tensile strength of decayed building materials by application of consolidating materials can indirectly reduce their deterioration due to physical-mechanical processes, such as ice and salt damage. However, the goal of consolidation is restoring the cohesion of decayed materials and not preserving them from future deterioration processes, hence alternative strategies have been explored to mitigate salt damage. Of course, controlling the environmental conditions (T and RH) and eliminating water sources (first of all, capillary rise) can help reduce damaging of walls. However, it is impossible to control temperature and relative humidity in outdoors environment and also the elimination of rising damp is definitely challenging (Flatt, 2002; Franzoni, 2014; Franzoni, 2018; Andreotti et al., 2019). In fact, although there are different methods to prevent rising damp, many of these methods are not fully effective and compatible, or simply are difficult to apply in historic structures (Franzoni, 2014). Some interventions, such as the use of hydrophobic treatments or the application of scarcely porous layers on the masonry surfaces, are even counterproductive, leading to a higher rise of damp and, often, to more severe damage caused by moisture and salts (Franzoni, 2014).

Several studies have focused on the use of modifiers of salt crystallization, which can act during both steps of the crystallization process (nucleation and growth of crystals) and can be distinguished in two different groups: inhibitors and promoters (Rodriguez-Navarro et al., 2002; Granneman et al., 2019; Bracciale et al., 2020). Crystal nucleation inhibitors are modifiers that increase the degree of supersaturation necessary to allow for the nucleation of crystals, thus increasing the time between the formation of supersaturation condition and the crystallization of salt. This results in the transport of the supersaturated salt solution over longer distances, thus favoring the formation of efflorescence rather than more harmful subflorescence. On the other hand, at higher level of supersaturation, if conditions for crystallization of the supersaturated solution occur, more severe damage will be experienced (Granneman et al., 2019; Bracciale et al., 2020). Crystal growth inhibitors are modifiers that retard crystal growth, covering the whole crystal surface and preventing the addition or the detachment of salt units (Granneman et al., 2019). Nucleation promoters work in the opposite way, increasing the salt nucleation rate that occurs at lower supersaturation (near or at the saturation condition), thus causing less damage to the substrate (Granneman et al., 2019). Different substances were tested in the last years as crystallization modifiers, like ferrocyanides (Rodriguez-Navarro et al., 2002; Selwitz and Doehne, 2002; Lubelli and van Hees, 2007; Rivas et al., 2010; Gupta et al., 2012) as inhibitors for sodium chloride, phosphonates (Lubelli and van Hees, 2007; Ruiz-Agudo et al.,

2012) as inhibitors for sodium sulphate and borax (Smith et al., 2010; Granneman et al., 2017) as promoter for sodium sulphate, just to name the most promising ones. A different strategy, adopted for example in (Houck and Scherer, 2006), is based on eliminating the crystallization pressure between the growing salt crystal and the inner pore wall by deposition of a thin polymeric layer. If the material surface could be modified so that the salt crystal does not repel it, the crystal itself would be able to grow in direct contact with the pore wall: in this case, the liquid film will not be maintained and, therefore, no pressure or damage will be generated in the material (Houck and Scherer, 2006). All of these products have different effectiveness and give different results depending on the type of salt, the porous substrate on which they are applied, the concentration used, etc., so that an improvement in the resistance to salt crystallization is usually found, but sometimes an increase in damage is experienced. The development of these crystallization modifiers is still mostly in the experimental phase, with many laboratory tests and few onsite applications, so more studies seem necessary (Granneman et al., 2019; Bracciale et al., 2020). In recent years, biomass-derived inhibitors were developed for the prevention of salt crystallization damage caused by different types of salt, focusing mainly on sodium sulphate and sodium chloride due to their destructive potential. It is the case, for example, of phosphocitrate, that was already tested with good results on different materials in laboratory and in the field (Cassar et al., 2008; Franceschini et al., 2015; Bracciale et al., 2020). These products, besides being derived from renewable sources, are non-toxic and usually soluble in water and/or alcohol, thus avoiding the use of harmful solvents (Bracciale et al., 2020), giving benefits to environment and human health. It is in this perspective that, in the present paper, a new bio-based protective material against salt crystallization (chitosan) was employed to improve the resistance of two porous carbonate stones to salt damage, alone and combined with a recently developed consolidant (hydroxyapatite). The present paper follows a previous preliminary study, in which this combined treatment was proposed for the first time, with encouraging results (Andreotti et al., 2019). An overview of the main properties of hydroxyapatite and chitosan is provided in the following.

Since more than a century, various organic and inorganic consolidating materials have been proposed for stone and other porous materials, with different results. Among these, the use of hydroxyapatite (HAP) and other calcium phosphate phases (CaP) has been studied since 2011 for consolidation and protection of carbonate stones (Sassoni et al., 2011). The CaP-based treatment has high potential because it provides significant mechanical consolidation in a short time, without altering porosity or transport properties of the substrate (Naidu et al., 2011; Sassoni et al., 2011; Sassoni et al., 2016a; Sassoni et al., 2016b; Sassoni, 2018). Hydroxyapatite, which is the main inorganic constituent of human teeth and bones, is a good consolidant for carbonate substrates as it is much less soluble than calcite and, at the same time, has a similar crystalline structure (Sassoni et al., 2011). As reported in the literature, the formation of HAP *in situ* is expected to occur by reaction between a carbonate-rich substrate, which provides calcium ions through dissolution, and an aqueous solution of a phosphate salt, usually diammonium hydrogen phosphate ($(NH_4)_2HPO_4$, indicated as DAP), which provides PO_4^{3-} ions (Naidu et al., 2011; Sassoni et al., 2011; Sassoni, 2018), according to the following reaction:

$$10CaCO_3 + 5(NH_4)_2HPO_4 \rightarrow Ca_{10}(PO_4,CO_3)_6(OH,CO_3)_2 + 5(NH_4)_2CO_3 + 3CO_2 + 2H_2O$$

One of the advantages of the use of the DAP-treatment is that all the by-products of the reaction, i.e., ammonium carbonate, carbon dioxide and water, are innocuous and volatile and, therefore, unwanted residues are not expected to remain in the stone.

In very recent years, the use of natural and biodegradable substances, mainly biopolymers, has been proposed in the field of conservation of building materials, as well as in other sectors. The idea backgrounding this new class of conservation materials is that they can potentially provide some interesting properties for a certain number of years, then naturally disappearing without leaving unwanted residues (Ocak et al., 2009; Ocak et al., 2015; Pedna et al., 2016; Andreotti et al., 2018). This requires that the treatment is applied again after some years, during maintenance works, but it also involves some advantages in comparison with traditional polymers used in conservation for many decades. In fact, traditional polymers are subject to unavoidable aging processes and performance loss in a limited number of years, but they are also hard to remove once they transformed during aging (by cross-linking, chain scission, crystallization, oxidation, etc.), thus influencing, and sometimes jeopardizing, the possibility to re-treat the materials with new consolidating and/or protective substances. In fact, the application of different polymeric treatments to heritage materials caused severe problems during last decades. In this context, some biopolymer-based water-repellents have been proposed (Ocak et al., 2009; Ocak et al., 2015; Pedna et al., 2016; Andreotti et al., 2018) for the protection of heritage materials against rain absorption, and chitosan was proposed as a treatment to fight salt damage (Andreotti et al., 2019).

Chitosan is already widely used in agriculture, in food sector, in environmental protection and in various biomedical applications, where its antibacterial and antioxidant properties are exploited (Muxika et al., 2017). Chitosan is produced from chitin, a marine origin polysaccharide that is widely available, being the second most abundant natural polymer after cellulose (Muxika et al., 2017; Philibert et al., 2017). Chitin is the main structural component in the exoskeleton of marine invertebrates and insects, as well as molluscs and crustaceans. When combined with calcium carbonate, like in shells of crustaceans and insects, chitin produces a strong composite, exhibiting improved hardness and stiffness compared to pure chitin and also a greater tenacity and ductility than pure $CaCO_3$ (Muxika et al., 2017; Andreotti et al., 2019). Chitin is a linear polysaccharide, consisting in N-acetyl-D-glucosamine units, connected by β—1.4 bonds (Muxika et al., 2017; Philibert et al., 2017; Andreotti et al., 2019), which is mostly obtained from industrial waste in the processing of marine shells, shrimps and similar, hence it is abundantly available. Despite its outstanding characteristics such

as biocompatibility, biodegradability and high mechanical strength, its exploitability is limited by its very low solubility (Muxika et al., 2017; Philibert et al., 2017; Andreotti et al., 2019). This turns the attention to chitosan, the main derivative of chitin. Chitosan is a copolymer obtained from the alkaline deacetylation of chitin, a process involving the treatment of chitin with hydroxides at high temperature. It consists in D-glucosamine and N-acetyl-D-glucosamine units, connected by β—1.4 glycosidic bonds (Muxika et al., 2017; Philibert et al., 2017; Andreotti et al., 2019). The ratio between the two units is called degree of deacetylation: for values ≥50%, chitosan becomes soluble in acidic media and, in this case, the aminic groups and the polymer become cationic, allowing them to interact with different molecules. This positive charge is believed to be responsible for its antimicrobial activity, allowing it to interact with negatively charged cellular membranes of microorganisms (Muxika et al., 2017).

The research in (Andreotti et al., 2019) was the first example of study on the behavior and the effects of chitosan applied to porous building materials. The study addressed prevention of salt crystallization damage by covering the pore surface with a chitosan coating, which can inhibit salt crystallization inside the pore network of the material. Chitosan was selected for some interesting properties: presence of functional groups in the molecular structure, acting as anchoring groups towards the mineral surfaces; film-forming capacity, to generate a continuous coating on the pore walls; highly flexible chains that allow for the interaction with any type of salt. Moreover, this polymer is not hydrophobic and does not alter the water transport properties of the treated substrate, which is beneficial for salt damage resistance and for preventing other deterioration processes (Houck and Scherer, 2006). In addition, it is bio-based and biodegradable, thus providing a minimum toxicity and complying with the new concept of "reversibility of treatment" explained above. Three different experimental setups were used in (Andreotti et al., 2019) and the results are briefly reported in the following. A first crystallization test was carried out by cooling a saturated aqueous solution of sodium sulphate and chitosan, showing that the polymer has a strong inhibiting effect on the salt crystallization, basically blocking it up to 2 °C, while in absence of chitosan salt crystallization occurred at 13.1 °C. The fact that chitosan inhibits sodium sulphate crystallization in the solution is thought to be due to its polyelectrolytic nature, providing a high number of positively charged sites that sequester sulphate ions. However, it was also reported that some polymers that inhibit salt crystallization when in solution might favor it when they are adsorbed on a solid surface, due to some polymer chain orientation (Ruiz-Agudo et al., 2006), so this aspect was specifically taken into account. A second test was carried out on different powdered substrates treated with chitosan. The powders, thanks to their large specific surface, allowed to demonstrate the remarkable film-forming ability of chitosan, which was adsorbed on the solid surface, creating a coating. Notably, the DAP-based consolidating treatment, applied before the polymer, caused an increase in the amount of chitosan adsorbed, probably thanks to the roughness of CaP phases that act as anchoring surfaces. When subjected to water flow, the treated powders (both with and without the DAP pre-treatment) exhibited initial solubilization of the thick chitosan layer, after which the adsorbed polymer was not further leached in water. In the final test, limestone samples were treated to investigate whether the inhibiting effect of chitosan observed in solution actually delay salt crystallization inside the stone, thus promoting formation of efflorescence over the surface, rather than development of mechanical stress inside the stone. While the polymeric treatment alone caused greater damage in the samples compared to the untreated references, as the retarding action of chitosan caused a higher supersaturation degree and a greater crystallization pressure in the zones of the pore walls not covered by the chitosan film, in the samples treated with DAP and then chitosan there was a remarkable benefit, with promotion of efflorescence and increase in the resistance to degradation.

While a preliminary evaluation of the adhesion and thickness of the investigated coatings on controlled, flat and non-porous surfaces of calcite and silica, and on powders of the two minerals, was carried out in the previous study with encouraging results (Andreotti et al., 2019), this paper focuses on the performance of the treatments in real stones, selecting two different salt crystallization tests aimed at producing a less drastic and hence more easy-to-interpret deterioration in the stone, with respect to the previous study. The two tests were carried out in order to consider two different mechanisms presently adopted to reproduce the damage by salts in laboratory, namely salt crystallization cycles and "wick effect". In this frame, it was decided to use the same shape of the samples adopted in the relevant standards and literature papers, i.e., cylinders for salt crystallization cycles (EN 12370, 1999) and prisms for the "wick test" (Goudie, 1986).

Starting from the preliminary findings briefly summarized above, the present study aims at further investigating the behavior of chitosan, by applying it to different substrates. In addition to the polymeric treatment alone, pre-treatment by DAP (followed by chitosan application) and treatment by DAP alone were also tested. The CaP phases that form in the material after the DAP treatment have been shown to provide good consolidating effectiveness, thus providing some benefits also in terms of resistance to salt crystallization pressure. Moreover, in the double treatment (DAP solution followed by chitosan), the CaP layer is expected to provide a good anchorage for the formation of a more homogeneous and defect-free polymeric layer, and also to protect calcite from dissolution in both neutral and slightly acidic water (Sassoni, 2018), thus preventing possible washout of the coating, which could cause a loss of effectiveness (Andreotti et al., 2019).

MATERIALS

Stones

The lithotypes chosen for this research are two types of bioclastic limestone, widely used in historic architecture of specific geographical areas, but also representative of porous carbonate stones used in many countries.

The first one is Globigerina limestone (labeled as "G"), which had been used also in the cited preliminary study (Andreotti et al., 2019). This stone is the major lithotype of the island of Malta, widely used in historic architecture and subject to severe deterioration by atmospheric agents and salts, leading to alveolization, flaking and pulverization (Sassoni et al., 2016a). It is an organogenic limestone composed mainly of calcite (about 95%), with traces of quartz and other impurities, and having a yellow-cream color.

The second lithotype was Lecce stone (labeled as "L"), a limestone used in southern Italy and, in particular, in Salento, which was chosen because it is similar to Globigerina limestone, but different enough to verify the repeatability of the results on a different substrate. Lecce stone is an organogenic limestone too, yellow-greyish in color, with a quite homogeneous composition based on calcite (about 95%), including a strong presence of marine fossils of different sizes, and a minor presence of phosphatic minerals (fluorapatite). The nature of this stone, as well as that of Globigerina limestone, makes it very vulnerable to deteriorating agents and salts in particular (Calia et al., 2013).

The slabs of Lecce stone from Cursi-Zollino-Melpignano quarry, Lecce (supplied by Décor S. r.l.) and the slabs of Globigerina limestone from the Qrendi area, Malta (Franka type, supplied by Xelini Skip Hire and High-up Service), were cut into eight prisms ($3 \times 3 \times 25$ cm^3, the longest side cut parallel to the stone bedding planes) and 21 cylinders (5 cm in diameter, 5 cm in height, core-drilled perpendicular to the bedding planes). The samples were gently washed with deionized water and placed in an oven at 60 °C until constant weight, then cooled to room temperature. Cylinders and prisms are indicated with the letters "C" and "P", respectively, following the letter indicating the type of stone (L_C, L_P, G_C, G_P).

Treatments

In the light of previous literature studies, where the application of DAP-based solutions was tested on different substrates, adopting different DAP concentrations and different additional compounds (Naidu et al., 2011; Sassoni et al., 2011; Franzoni et al., 2015; Sassoni et al., 2016a; Sassoni et al., 2016b; Sassoni, 2018), a solution containing 0.1 M DAP + 0.1 mM $CaCl_2$ in 10 vol % ethanol was used in the present study. DAP, $CaCl_2$?$2H_2O$ and ethanol were purchased from Sigma-Aldrich (reagent grade). A low concentration of DAP is preferable to avoid formation of a too thick film over the pore surface, which would more prone to cracking during drying, as well as to prevent formation of metastable CaP phases and the possible persistence of unreacted DAP in the treated stone. Because the lower the DAP concentration, the lower the amount of PO_4^{3-} ions necessary to form HAP, ethanol and $CaCl_2$ were added to the DAP solution. Ethanol exerts a weakening action on the hydration sphere of phosphate ions in solution and hence promotes formation of CaP (Graziani et al., 2016; Sassoni et al., 2018), while $CaCl_2$ guarantees a better surface coverage by providing additional calcium ions, also preventing excessive dissolution of the substrate (Naidu and Scherer, 2014).

For the polymeric treatment, based on the results obtained in (Andreotti et al., 2019), a 0.05 wt% chitosan solution was prepared. As mentioned in the Introduction, chitosan can be solubilized only in acidic media. For this reason, the pH of the solution was brought to ~3 with the addition of acetic acid, which was chosen because it does not leave any unwanted components in the solution. Once the chitosan was completely dissolved, the solution was brought back to neutrality (pH between six and 7), not to damage the stone substrate. pH adjustment was obtained by adding 15 ml of a 0.03% NaOH solution to 1 L of chitosan solution.

The labels and number of specimens per type of treatment are summarized in the following:

- two cylinders for each lithotype were not treated, remaining as reference material (labeled as "UT");
- two prisms and three cylinders for each lithotype were not treated and were subjected to the crystallization tests (labeled as "UT_SALT");
- two prisms and five cylinders for each lithotype were treated only with the chitosan solution (labeled as "CHIT"). Except for two cylinders, which were left non-degraded, all these samples were subjected to the crystallization tests ("CHIT_SALT");
- two prisms and five cylinders for each lithotype were treated only with the consolidating solution (labeled as "HAP"). Except for two cylinders, which were left non-degraded, all these samples were subjected to the crystallization tests ("HAP_SALT");
- two prisms and six cylinders for each lithotype were treated first with the consolidating solution and then with the chitosan one (labeled as "HAP + CHIT"). Except for two cylinders, which were left non-degraded, all these samples were subjected to the crystallization tests ("HAP + CHIT_SALT").

METHODS

Characterization

The main characteristics of the stones used in the research were first investigated. The values of bulk density, open porosity and dynamic elastic modulus were measured not only in the untreated stone specimens, but also in subsequent phases, to check the effectiveness of the treatments and the extent of degradation induced by the salt crystallization tests.

The bulk density, ρ_g [g/cm^3], of the stone samples was determined as the ratio of dry mass over volume, as average for all the specimens. The size of the specimens was measured with a caliper and the dry mass was measured after oven drying at 50 °C until constant mass and cooling to room temperature.

Water absorption test was carried out according to (EN 15801, 2009) on three cylinders (UT) of each lithotype and on all the prisms. The samples were placed vertically on a filter paper pack partially immersed in deionized water, checking that the water level did not exceed the height of the filter paper, so that the samples absorbed water by capillarity only from the base surface. The samples were weighed at increasing time intervals for a total of 24 h. The capillary water absorption coefficient, AC [kg/m$^2\sqrt{s}$], is represented by the slope of the first linear part of

the curve, and the total water absorption after 24 h, WA_{24hrs} [wt %], is calculated as follows: $WA_{24hrs} = (W_{24hrs}–W_{dry})/W_{dry}$. This test was carried out on two cylindrical replicates for each treatment too (CHIT, HAP, HAP + CHIT), to evaluate if and how much the treatments altered the transport properties of the materials. In fact, porosity and transport properties are fundamental aspects to consider when investigating the crystallization of any saline solution. Moreover, any treatment in the conservation of heritage materials is required to cause very limited porosity alterations, to avoid damages and defects both in short and long time.

Tensile splitting test was carried out on cylinders after the salt crystallization cycles (2 replicates for each condition) and on UT samples, to determine the tensile strength σ_t [MPa] of the stone before and after degradation. In fact, salt degradation leads to a loss of cohesion between the stone particles, the detachment of an outer layer and the formation of internal micro-fractures: this leads to decrease in the tensile strength of the material. Consolidating substances, such as hydroxyapatite, are applied to restore the cohesion between the particles and bring back the tensile strength of the stone to its original value, thus increasing its resistance to degradation. For this reason, the splitting test on degraded samples is an indication of the effectiveness of the treatments applied. The test was carried out using an Amsler-Wolpert loading machine (maximum load 20 kN) at a constant displacement rate of 4 mm/min and cardboard couplers (1 mm thick) to allow for uniform compression along the sample. Before carrying out this test, the lateral surface of the samples was gently scratched with fine sandpaper to remove any possible protuberances.

Open porosity and pore size distribution of the two stones were determined by mercury intrusion porosimetry (MIP), using a Thermo Scientific Pascal 140 (macropores unit) and a Pascal 240 (micropores unit). In particular, two fragments of each lithotype were analysed, about 1 g in weight. This analysis was performed also on the treated and the salt deteriorated samples, collecting one fragment for each condition from cylindrical samples, to analyse the changes in porosity. The fragments of the salt deteriorated samples (described in § 4.2.1) were taken close to the top surface of the cylinders (at the center of such surface), excluding the external salt crust. Before the analyses, these fragments were desalinated with a poultice of cellulose pulp and deionized water (weight ratio 1 : 4), which was wrapped in a PE film and left to act for 24 h. Afterwards, the film was removed and the poultice was allowed to completely dry. Desalination was carried out to remove the salt crystals deposited in the pores, thus allowing to investigate the variation of the stone porosity due to deterioration of only.

The external surface of untreated and treated samples was observed using a Philips XL20 SEM scanning electron microscope (SEM), equipped with energy dispersive spectrometry (EDS, EDAX probe). The sample surface was made conductive by sputtering with aluminum before SEM observation.

The dynamic elastic modulus E_d [GPa] was measured on the cylinders before and after treatments, and on the prisms at each stage of the research. Ultrasonic tests for the determination of dynamic elastic modulus were carried out with a Matest instrument, with 55 kHz transducers and rubber couplers to improve the contact between surfaces. For cylinders, the measurement was performed across the height of each sample, while for prisms 10 elastic modulus values were measured for each sample, i.e., at 4 cm intervals along the height of the prism and in two orthogonal directions. In fact, as the prisms are 25 cm high, they could exhibit internal inclusions (for example, fossils in Lecce stone), causing a certain degree of heterogeneity and variability of the values. The dynamic elastic modulus for the prisms was obtained averaging all the 10 values obtained for each sample and the two samples of each condition. For the prisms, E_d was measured in the original stone specimens, in the samples treated with consolidant and/or polymer, in the samples deteriorated by the salt crystallization test and in these latter samples after desalination. In fact, after the salt crystallization cycles, the prisms where subjected to three desalination procedures, by using the same poulticing method described above. Before any E_d measurement, the samples were dried in oven at 50 °C for 24 h.

Treatment Procedure

Both consolidating and biopolymeric solutions were applied to stone samples by capillarity. In the case of the consolidant, four prisms and 11 cylinders of each lithotype were placed in vessels under a 5 mm solution head, the prisms lying on a lateral face to allow for a better absorption. For the first 2 h, necessary refills were carried out and then, when the samples appeared completely wet, the vessels were covered, and the samples were left to absorb the solution up to a total of 24 h. Afterwards, a quick washing under deionized water was carried out, to eliminate unreacted DAP and any possible surface patina, and the samples were dried in room conditions until constant weight. The biopolymeric treatment was applied according to the same procedure. In particular, the chitosan solution was applied to two prisms and five cylinders of untreated stone and two prisms and six cylinders of stone that had been previously treated with the DAP-based consolidating solution and left to dry.

After each treatment application and subsequent drying, the samples were weighed to determine their weight increase, an indication of the amount of hydroxyapatite and/or polymer deposited in the stone. The dynamic elastic modulus was measured again on treated samples, after drying. The weights and the dynamic elastic modulus values were averaged for the five replicates of UT, CHIT and HAP cylinders, the six replicates of the HAP + CHIT cylinders and the two prismatic replicates of each type.

Crystallization Tests

Sodium sulphate is normally used for accelerated weathering tests in laboratory because it is one of the most harmful salts in nature (Rodriguez-Navarro et al., 2000; Tsui et al., 2003; Steiger and Asmussen, 2008; Espinosa-Marzal and Scherer, 2009; Flatt et al., 2014). The peculiarity of this salt is its capacity to crystallize in eight different forms and, above all, to have two phases that can crystallize at normal environmental temperature and humidity: thenardite (anhydrous phase) and mirabilite (decahydrate phase) (Steiger and Asmussen, 2008; Flatt et al., 2014). The greatest

damage occurs when thenardite is dissolved and mirabilite precipitates: in this case, during the dissolution of thenardite, a solution highly supersaturated with respect to mirabilite is formed, which causes a strong crystallization pressure inside the material when mirabilite precipitates, which occurs with a large volumetric expansion (about 314%) (Flatt, 2002; Espinosa-Marzal and Scherer, 2009).

An accelerated salt deterioration test procedure is proposed in the European standard (EN 12370, 1999). This procedure involves cycles of total immersion in a saturated (14 wt%) sodium sulphate decahydrate solution for 2 h, followed by oven drying at 105 °C for at least 16 h and finally cooling to room temperature. For each new cycle, new saline solution with the same concentration is used, which leads to the accumulation of a very high amount of salt inside the samples. This procedure results extremely aggressive towards materials and it is not considered very representative of real salt damage mechanisms occurring in historic buildings (Lubelli et al., 2018), both due to the impressive amount of salt accumulated and high drying temperature. For this reason, a 14 wt% sodium sulphate decahydrate solution was used for the present crystallization tests, as in the EN standard, but it was decided to slightly modify the testing procedure.

In a first type of crystallization test, the cylindrical samples of both lithotype (3 replicates for UT, CHIT and HAP and four replicates for HAP + CHIT) were subjected to cycles of impregnation, followed by drying. During the first cycle, the samples were impregnated by partial immersion in the saline solution. The samples, divided according to the lithotype and type of treatment, were placed in separate vessels with 400 ml of saline solution and the solution level (about 5 mm) was kept constant by refilling with deionized water. The impregnation phase lasted 4 h, followed by drying for 44 h in laboratory conditions (T = 20–25 °C, RH = 45–80%). In all the subsequent cycles, the wetting phase (4 h) was carried out using deionized water only, in order to keep the total salt amount in the samples constant and to induce salt accumulation at the upper surface. After each drying phase (44 h), the samples were gently brushed to remove both efflorescence and debris or powder detached from the substrate. For each cycle, the samples were weighed at the end of the immersion phase (W_{wet}) and twice at the end of the drying phase, before and after brushing (W_{dry} and $W_{dry,\ brushed}$). All these values were averaged for the samples of the same group. A total of 12 cycles was carried out following this procedure. After 12 cycles, the samples were still in good conditions, probably due to a too limited aggressiveness of the procedure adopted. In fact, the brushing of the efflorescence after each drying phase likely reduced the amount of salt present inside the samples and, moreover, the high air RH present in some drying phases may have prevented the complete drying and the transformation of mirabilite into thenardite, limiting the damage in the subsequent rewetting. Thus, it was decided to carry out further eight cycles, each lasting 24 h and consisting of 4 h of capillary absorption of deionized water, 18 h of oven drying at 50 °C (temperature chosen not to damage the polymeric coating) and 2 h of cooling in room conditions. In this way, the oven drying, with RH varying between 8 and 12%, certainly caused formation of thenardite at each cycle and the subsequent formation of mirabilite in the wetting phase, leading to the ideal conditions for the occurrence of a more severe damage. The brushing phase and the weight measurements at each cycle remained the same.

In a second type of crystallization test, two prismatic samples for each condition were subjected to continuous capillary absorption of the saline solution with concomitant evaporation, a condition called "wick effect" (Goudie, 1986; Andreotti et al., 2019), which reproduces the typical salt supply that occurs during capillary rise from the soil in a real building. Each sample was placed vertically in a beaker filled with 200 ml of 14 wt% sodium sulphate decahydrate solution (height of immersion: 5 cm). To prevent evaporation from the free surface of the saline solution, a layer of melted paraffin was poured over the solution: after solidification, the paraffin adhered to the sample and the beaker, preventing evaporation. The samples were placed in a climatic chamber at T = 22 ± 0.5 °C and RH = 80 ± 2%. The test ended when the solution was completely absorbed by the samples and evaporated from their surface, which happened after 5 days for G and 7 days for L. The slightly different drying times for the different samples and treatments were probably due also to the morphology and thickness of the layers of efflorescence on the samples surface. After drying, the samples were gently brushed to remove efflorescence and debris and placed in an oven at 60 °C until complete drying, and finally weighed ($W_{dry,\ brushed}$). Considering that all the prisms were still in good conditions, it was decided to repeat this same test again, on one sample for each type.

The debris obtained after the first continuous absorption test were collected separately for each type of samples, then they were firstly dried in oven at 60 °C for 24 h and then cooled to room temperature in a desiccator. Once dry, they were put in boiling deionized water for 10 min and subsequently filtered, in order to extract the salt ions from the solid part (debris of stone). The saline solutions obtained were then analysed by ion chromatography (Dionex ICS 1000) to obtain the amount of sulphate anions and, by calculation, the percentage weight of solid fraction (ΔW_{solid}) and sodium sulphate (Na_2SO_4) fraction (ΔW_{salt}) referred to the initial weight of the samples.

RESULTS AND DISCUSSION

Characteristics of the Stones and Effects of the Treatments

The characteristics of stone cylinders before and after treatments are reported in **Table 1**, in terms of weight and elastic modulus variation, while the characteristics of stone prisms before and after treatments are reported in **Table 2**. The weight increases of the samples are almost negligible for all the treatments, due to the low concentration of the solutions applied, which is positive as it suggests that only a thin coating of the two substances formed over the pore surface, avoiding any pore clogging effect. For HAP + CHIT samples, due to the double treatment, the weight variation was slightly greater but, in any case, extremely limited. Interestingly, the weight increases due to chitosan application in the double treatment (HAP + CHIT) was lower with respect to

TABLE 1 | Characteristics of cylindrical samples: mass variation after treatment in dry condition (ΔW), dynamic elastic modulus before and after treatment (E_d), variation of dynamic elastic modulus (ΔE_d).

Substrate	Treatment	ΔW [g]		E_d [GPa]		ΔE_d [GPa]
		After DAP	After chitosan	Before	After	
L_C	CHIT		+0.22 ± 0.043	16.25 ± 3.278	17.01 ± 3.402	+0.76
	HAP	+0.23 ± 0.022		16.10 ± 2.932	16.56 ± 3.162	+0.45
	HAP + CHIT	+0.28 ± 0.059	+0.05 ± 0.027	18.27 ± 2.177	18.99 ± 2.210	+0.72
G_C	CHIT		+0.22 ± 0.055	13.76 ± 0.449	13.94 ± 0.457	+0.17
	HAP	+0.27 ± 0.019		13.67 ± 0.244	13.93 ± 0.083	+0.27
	HAP + CHIT	+0.33 ± 0.102	+0.02 ± 0.015	13.90 ± 0.268	14.04 ± 0.158	+0.13

TABLE 2 | Characteristics of prismatic samples: mass variation after treatment in dry condition (ΔW), dynamic elastic modulus before and after treatment (E_d), variation of dynamic elastic modulus (ΔE_d).

Substrate	Treatment	ΔW [g]		E_d [GPa]		ΔE_d [GPa]
		After DAP	After chitosan	Before	After	
L_P	CHIT		+0.63 ± 0.007	15.54 ± 0.109	15.86 ± 0.034	+0.33
	HAP	+0.55 ± 0.014		15.73 ± 0.288	16.79 ± 0.160	+1.06
	HAP + CHIT	+0.45 ± 0.127	+0.15 ± 0.057	15.70 ± 0.235	16.71 ± 0.164	+1.01
G_P	CHIT		+0.64 ± 0.014	13.08 ± 0.035	13.25 ± 0.118	+0.17
	HAP	+0.66 ± 0.007		13.06 ± 0.056	13.66 ± 0.052	+0.60
	HAP + CHIT	+0.72 ± 0.000	+0.12 ± 0.014	13.41 ± 0.084	13.89 ± 0.246	+0.48

the CHIT treatment alone, which was found also in a previous study (Andreotti et al., 2019). This aspect is probably related to the mechanism of adsorption of chitosan over different solid substrates (in this case, the layer of CaP phases), which may depend on several factors, including the chemical nature of the substrate, the pH of the solution, etc. (Andreotti et al., 2019), and which was not specifically investigated in the present study. It is also possible that the capillary absorption of the chitosan solution was somehow slowed down in the HAP-treated stone (see **Figure 1** below).

All the treatments also caused a systematic increase in the dynamic elastic modulus, although quite limited and difficult to distinguish from the intrinsic variability for this parameter in the two stones analysed. In fact, the elastic modulus of untreated Lecce stone and Globigerina limestone, averaged between all samples used, is 16.47 ± 2.756 GPa and 13.75 ± 0.345 GPa, respectively. The E_d increase reached a maximum of 0.72 GPa for Lecce stone and 0.27 GPa for Globigerina limestone (**Table 1**), hence within the respective standard deviations of the untreated value. The standard deviation of the dynamic elastic modulus for Lecce stone is quite high due to the presence of marine fossils within this stone and hence its heterogeneous microstructure. Both the weight increase and the E_d increase after treatments are generally slightly higher for prisms than for cylinders, owing to the smaller thickness of the first ones, which allowed a greater absorption of the solutions and deposition of HAP and/or chitosan in the stone.

The results of the water absorption test on the cylinders are shown in **Figure 1**, while the average values of capillary water absorption coefficients (AC) and the total water absorption at 24 h (WA%) are reported in.

Supplementary Table S1. The MIP curves of the samples with and without the treatments are reported in **Figure 2**.

After 24 h of capillary absorption, the samples were not completely saturated yet, as the slope of the last part of the curves in **Figure 1** is still slightly increasing. This is due to the presence of pores of different sizes within the material, as shown by the MIP analyses in **Figure 2**. The bigger pores are the first to absorb water and be saturated, later acting as reservoir for the thinner pores that could take a much longer time to be saturated. Nonetheless, in the untreated condition the capillary absorption was almost complete after 24 h. The total water absorption at 24 h and the total porosity are similar for the two stones, with slightly higher porosity for Globigerina limestone and slightly higher variability of results for Lecce stone, the latter due to the more heterogeneous microstructure of this lithotype. The AC coefficient of Globigerina limestone is higher than that of Lecce stone, consistently with its slightly higher porosity and larger pore mean radius found by MIP.

After treatments, all the samples exhibited similar total porosity and pore size distribution (**Figure 2** and **Supplementary Table S1**), and the differences are attributable to the intrinsic variability of the stones. Despite this, the treatments modified the capillary water absorption rate of the stones. In Lecce stone, all the treatments slowed down the water capillary absorption compared to UT samples, especially in the case of HAP and HAP + CHIT. In Globigerina limestone, slight variations in AC were registered after the CHIT and the HAP treatments, while the combined treatment HAP + CHIT caused a marked reduction in AC. The modification of the capillary absorption rate could suggest a pore clogging effect, but the variation in the pore size distribution is negligible, as shown

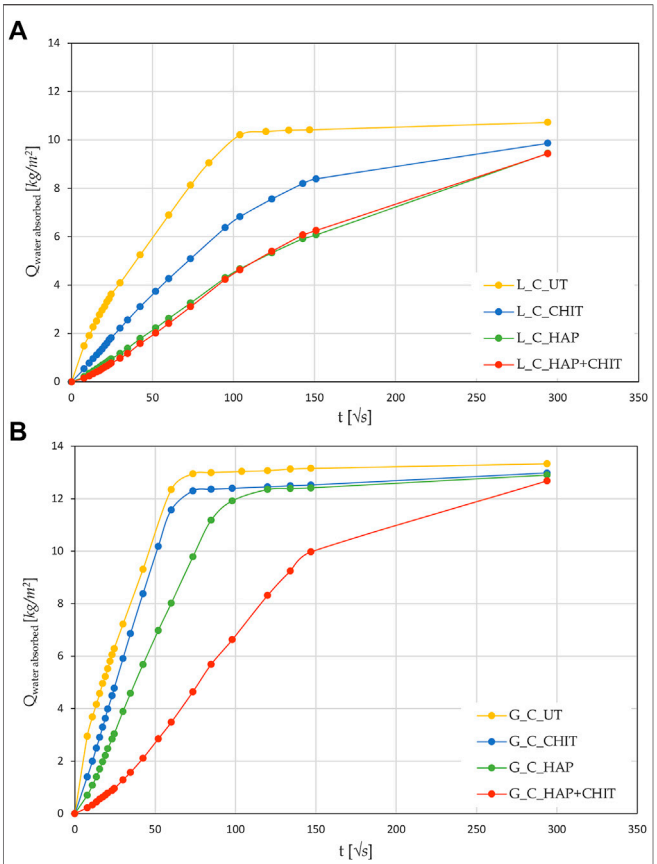

FIGURE 1 | Capillary water absorption curves for the untreated (UT) and treated cylindrical samples for **(A)** Lecce stone and **(B)** Globigerina limestone. Values are averages for at least two samples.

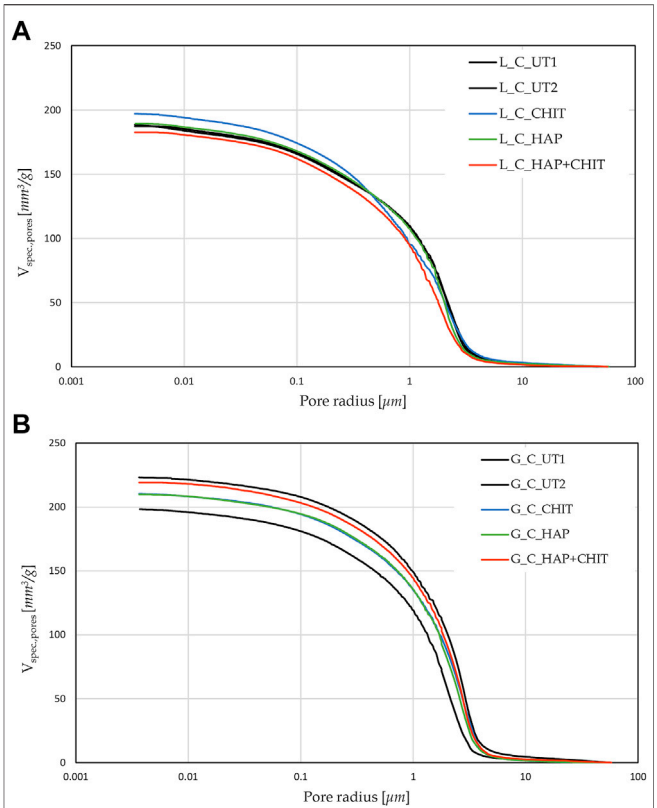

FIGURE 2 | Pore size distribution of various type of stone samples, obtained with MIP test, compared to the relative UT samples, for **(A)** Lecce stone and **(B)** Globigerina limestone.

in the results of MIP test (**Figure 2**), hence no significant pore occlusion occurred. The reduction of AC could be due to changes in the roughness of the pores surface after treatments and/or modifications in the contact angle with water. In the case of HAP-treated stone, changes in sorptivity comparable to those found in the present paper have been found in previous studies (Sassoni et al., 2011; Sassoni et al., 2016a), as a result of the moderate alterations in the static contact angle (Sassoni et al., 2016a; Sassoni et al., 2020) and in pore size distribution (Sassoni et al., 2011; Sassoni et al., 2016a).

Based on SEM images taken on the external surface of untreated and treated samples of Globigerina (**Supplementary Figure S1**), it is possible to observe that neither the single treatments (HAP or CHIT) nor the combined treatment (HAP + CHIT) led to formation of a clearly distinguishable coating over the stone surface. Accordingly, EDS analysis did not reveal any element that could be attributed to newly formed coatings (such as P in the HAP and HAP + CHIT coatings). Given the high porosity of the stone, the DAP and chitosan solutions were quickly absorbed into the pore network (thus leading to the changes in pore size distribution and water sorptivity discussed above), while no accumulation on the treated surface took place. The lack of coating accumulation on the surface was likely helped by rinsing with water at the end of the treatment application. The samples were rinsed with water to remove the excess of unreacted DAP (with chitosan possibly deposited on top) that accumulated on the sample surface, so as to prevent formation of a surface crust and pore clogging, with consequent alterations in the stone transport properties. Similar results were obtained also in the case of Lecce stone (SEM images are omitted for brevity's sake).

In any case, the present results suggest that:

- the AC modifications due to the three kinds of treatments are different in the two stones. In particular, the impact of the treatments is smaller in L than in G, probably due to the much quicker capillary absorption of the latter, which overcomes the possible microstructure modifications caused by the treatments;
- the same chitosan solution tested here, when applied as a coating over a glass slide, exhibited a static contact angle of about 65 °, i.e. much higher than stone, although still in the hydrophilic field (<90 °). This may explain the slower capillary absorption of L_CHIT and L_HAP + CHIT compared with the untreated Lecce stone. In the case of Globigerina limestone, having a much faster capillary absorption, the AC coefficient of the stone was almost unaltered by CHIT treatment, while it

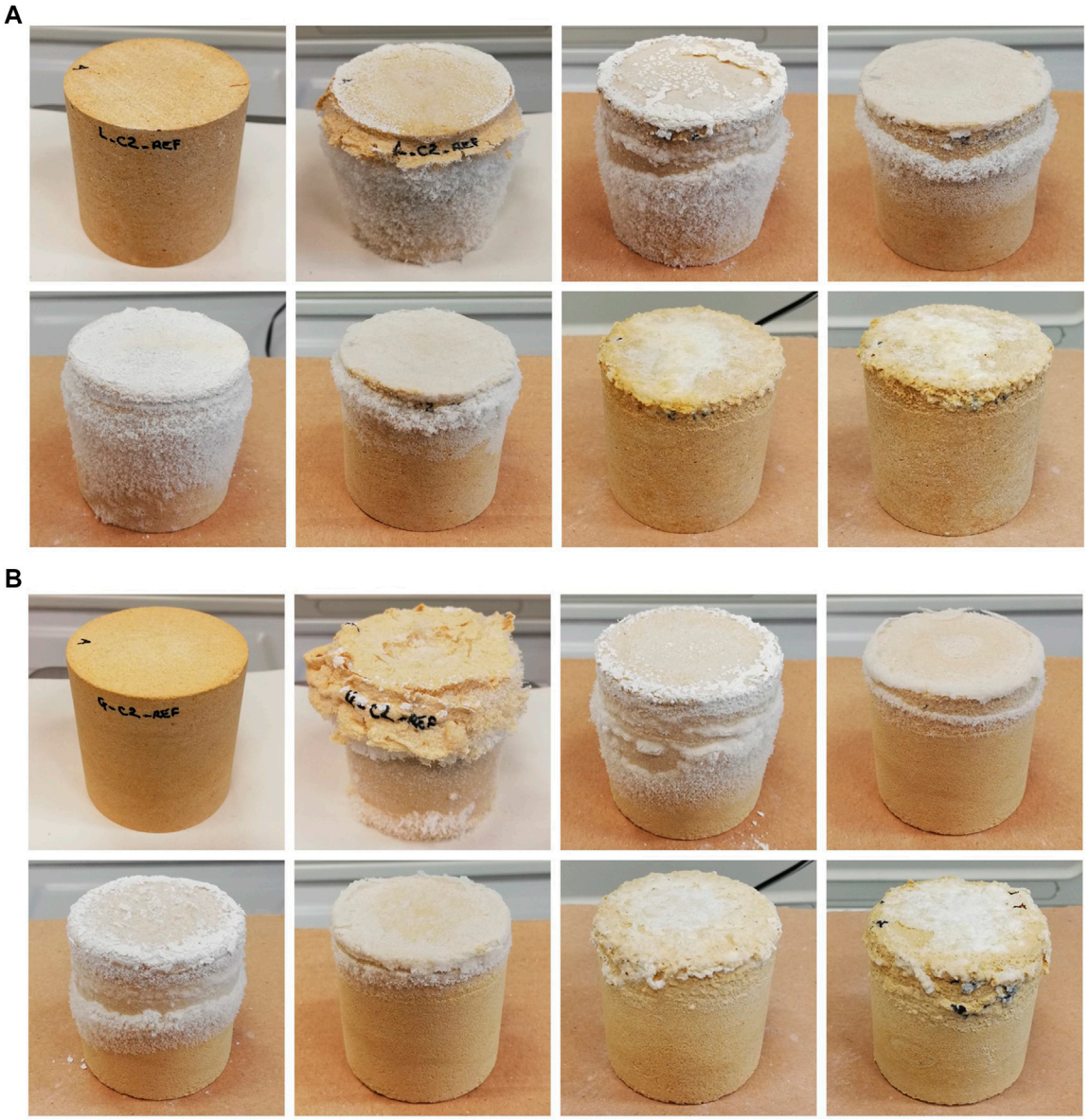

FIGURE 3 | Significant UT cylinders at the 1st, 2nd, 4th, 6th, 10th, 12th, 16th and 20th cycles of the salt crystallization test for: **(A)** Lecce stone and **(B)** Globigerina limestone. The photos were taken after the drying phase, before brushing.

decreased for the double treatment (G_HAP + CHIT), although less than in Lecce stone.

It is also possible that the slowing down of the capillary absorption rate found in the test is transitory, maybe related to some washout of the chitosan layer and/or of some unreacted DAP. In fact, in the previous study, the chitosan coating applied over calcite was found to be washed out by water until reaching the adsorbed layer, which in turn was not sensitive to water flow (Andreotti et al., 2019). Unfortunately, it was not possible to repeat the test on the same cylindrical samples, as they were broken and used for other analyses, hence this aspect will be investigated in future studies.

Effects of the Salt Crystallization Tests

Tests on Cylinders

The appearance of the untreated cylindrical samples during the 20 crystallization cycles (the first 12 carried out with drying at room temperature and the other 8 with oven drying at 50 °C) is reported in **Figure 3**, for some selected cycles and for one representative sample. At the end of the first cycle, no deterioration was found, as expected, because no thenardite to mirabilite transformation had taken place yet. It can be clearly observed that oven drying increased the aggressiveness of the crystallization cycles (see the photos of the 16th and 20th cycles in **Figure 3**), as expected. However, the untreated cylindrical samples were still in relatively good conditions even at the end of

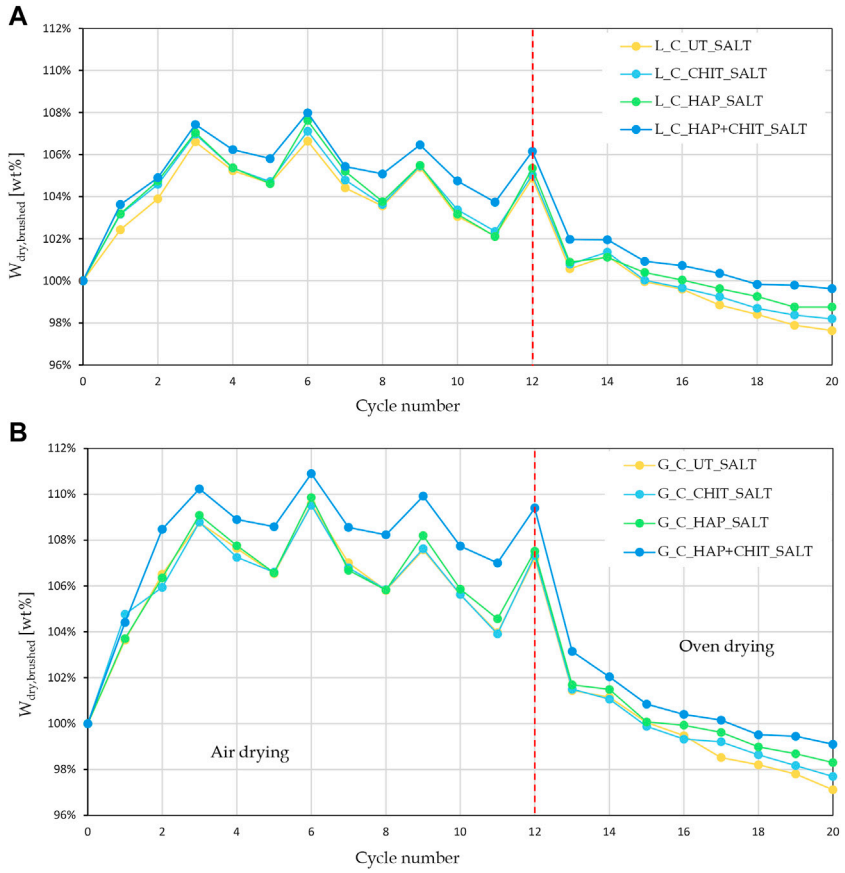

FIGURE 4 | Weight variation of the cylindrical samples after drying and brushing, at each cycle of the salt crystallization test for: **(A)** Lecce stone (UT and with different treatments) and **(B)** Globigerina limestone (UT and with different treatments).

the 20th crystallization cycle. The limited severity of the adopted testing conditions seems to be due to two main reasons:

- the saline solution was used in the first wetting cycle only, while deionized water was used in the following cycles. This means that a major amount of the salt that was introduced in the first absorption cycle was removed when efflorescence and debris were brushed away at the end of the first cycle and this amount was not re-introduced in the samples in the subsequent cycles. This is confirmed by the definitely more

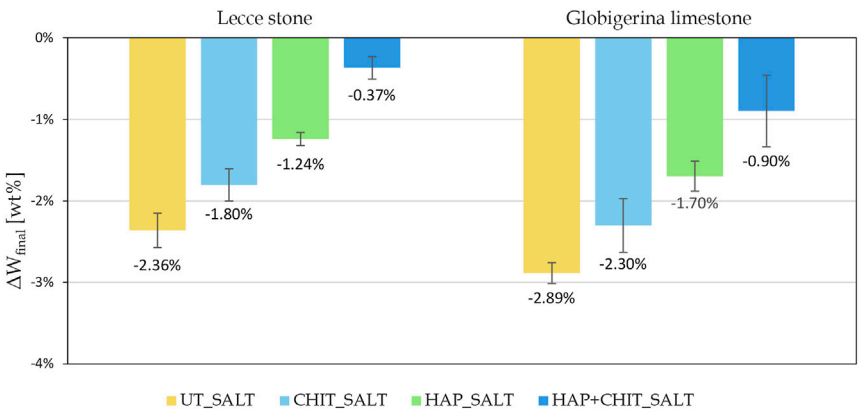

FIGURE 5 | Change in the final dry weight, after brushing, compared to the initial weight of the cylindrical samples.

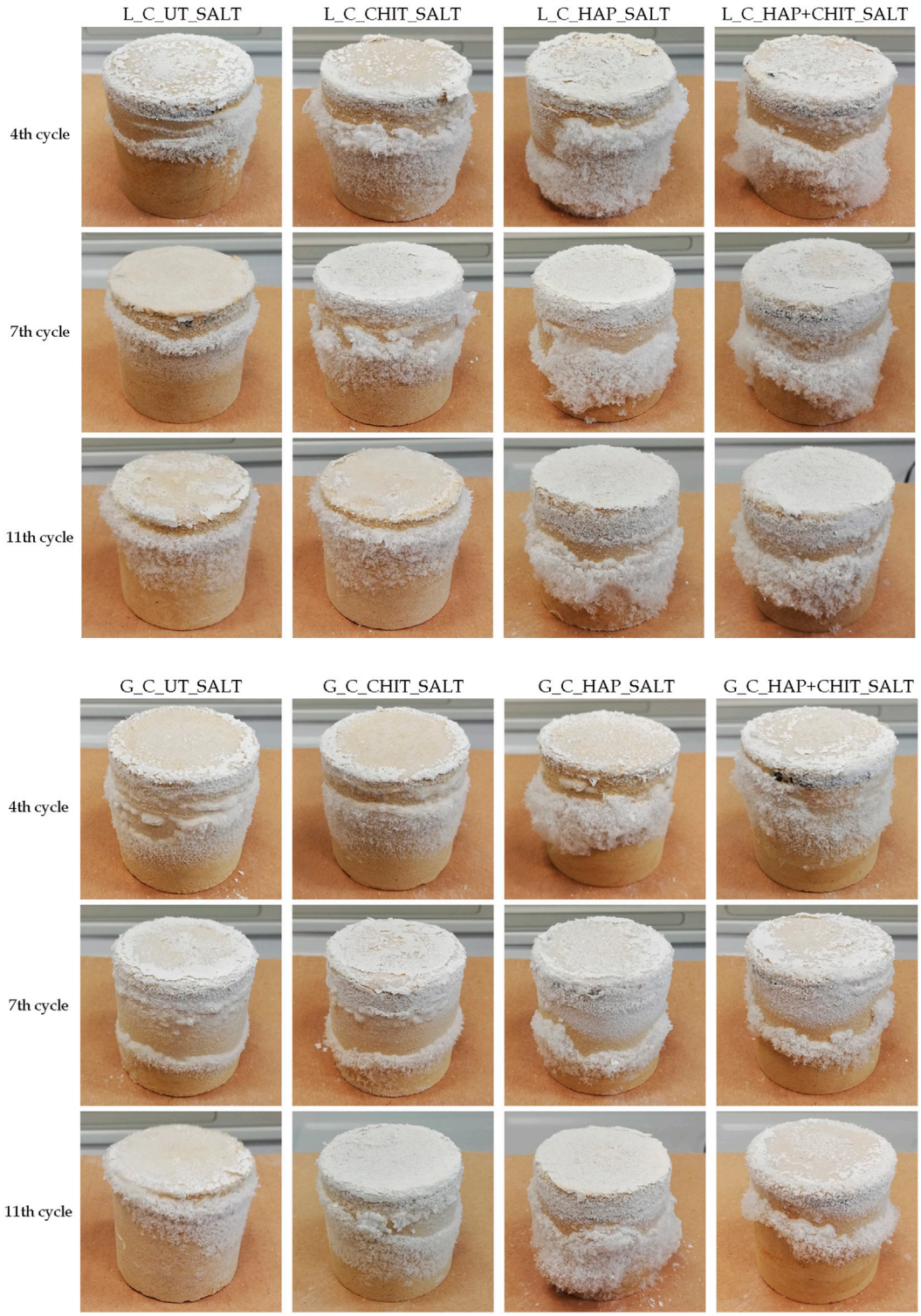

FIGURE 6 | Lecce stone samples and Globigerina limestone samples during the cycles (dried condition, before brushing), where the difference in the amount of efflorescence formed in the different type of samples can be seen. The pictures of the cycles with oven drying are not reported, because the "cementification" of debris during drying made impossible to distinguish the layer of efflorescence.

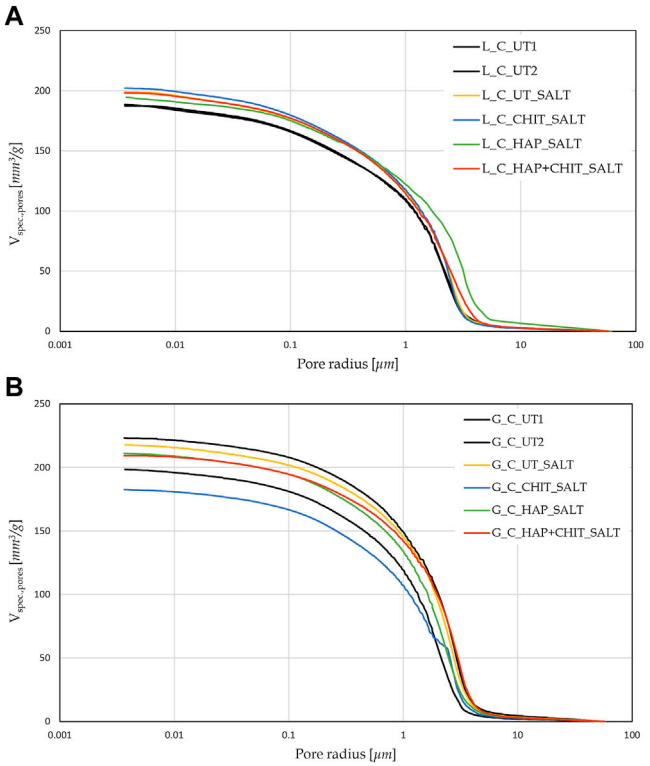

FIGURE 7 | Pore size distribution of stone samples, obtained with MIP test, after the salt crystallization test (and desalination by poulticing) for: **(A)** Lecce stone and **(B)** Globigerina limestone.

abundant salt crystals formation observed at the end of the second cycle (**Figure 3**), which was not found in the following ones;—the stone fragments that tended to detach during the wetting phase were apparently "cemented" by salt during the subsequent drying phase and this greatly limited the weight loss of the samples, making it difficult to quantify the actual degree of deterioration.

The weight variations of the samples after each drying + brushing phase ($W_{dry,\ brushed}$) are reported in **Figure 4**, while the variation of the final dry weight compared to the initial one (ΔW_{final}) is reported in **Figure 5**.

The graphs in **Figure 4** clearly indicate that the first part of the test, with drying at room temperature, led to a strong weight increase, with no apparent damage in the stones. This can be ascribed to the fact that the samples did not completely dry in laboratory conditions prior to the next wetting cycle, thus also preventing the transformation from mirabilite to thenardite and limiting the damage. Moreover, the peaks in the first part of the test suggest that the variations in the air RH at each drying cycle caused a variable degree of drying before the next wetting phase. Only in the second part, when oven drying was used, there was a continuous weight loss, below the initial weight of the samples. Concerning the effect of the treatments, it can be noted that the curves of the UT_SALT samples are the lowest in **Figure 4**, with a maximum weight loss (ΔW_{final}) equal to $-2.36 \pm 0.21\%$ for L and $-2.89 \pm 0.13\%$ for G (**Figure 5**). All the treatments improved the performance of the stones, the benefit increasing in the following order: UT ≈ CHIT < HAP < HAP + CHIT. The fact that the HAP treatment alone has a positive effect on the salt resistance of the stone can be ascribed to several factors, which act simultaneously: 1) an increase in the stone tensile strength (as suggested by the increase in the elastic modulus and as seen in the literature (Naidu et al., 2011; Sassoni et al., 2011; Sassoni et al., 2016a; Sassoni et al., 2016b; Sassoni, 2018)), with a consequent improvement in the salt resistance (Sassoni et al., 2016b); 2) the fact that a greater roughness of the pore surfaces allows for a better capillary flow towards the outside once this roughness is wet, promoting efflorescence (Scherer and Wheeler, 2008; Andreotti et al., 2019); 3) the preventive action towards calcite dissolution (Graziani et al., 2015; Sassoni et al., 2016a; Sassoni et al., 2016b; Andreotti et al., 2019). All these positive effects seem to add to those of chitosan in the samples with the double treatment, where the presence of the polymer helps reduce the stone degradation, by increasing the formation of external efflorescence compared to the UT samples (**Figure 6**). In fact, the HAP + CHIT_SALT samples exhibited a systematically lower weight loss at every cycle than all the other samples, which

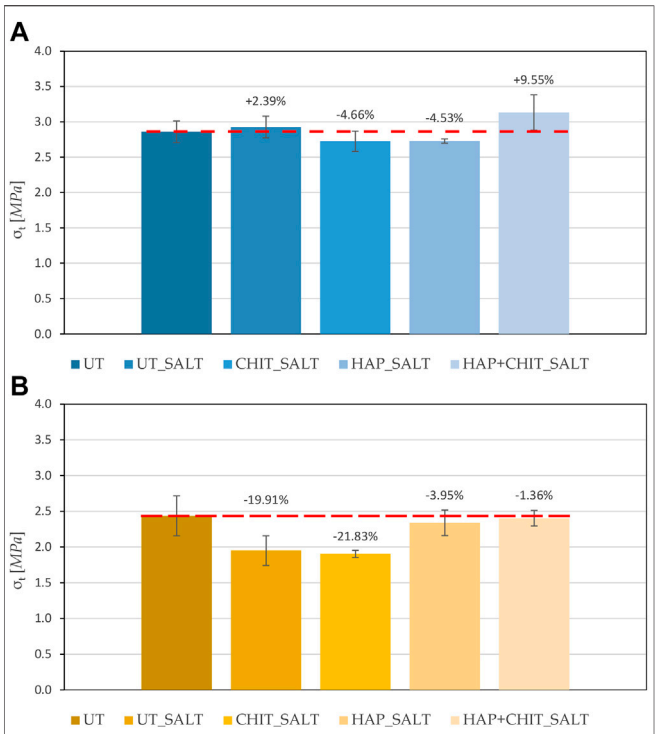

FIGURE 8 | Tensile strength of the cylindrical samples, obtained with splitting test, after the crystallization test and compared with the UT sample, for: **(A)** Lecce stone and **(B)** Globigerina limestone. The dotted line indicates the initial value of the UT reference (2.86 MPa for L and 2.44 MPa for G).

indicates better resistance to salt damage: at the end of the cycles, the HAP + CHIT treatment made the weight loss decrease by 84% in Lecce stone and by 69% in Globigerina limestone, with respect to the untreated samples. The polymeric treatment alone induced a behavior quite similar to the untreated samples, hence it seems that the inhibiting action of chitosan alone is not sufficient, or, most likely, the polymer is not well distributed and anchored to the pore surface. As a matter of fact, chitosan seems to promote the formation of efflorescence rather than subflorescence, as confirmed by the fact that the final weight loss of the samples is lower than that of the untreated samples. However, it is also possible that the inhibiting effect of chitosan causes a greater supersaturation of the saline solution inside the pores, which causes local stress concentrations in those areas of the pores surface that are not covered by the chitosan coating. In the case of HAP + CHIT, this problem was not found, as the CaP layer improved the coverage and the adhesion of chitosan.

The MIP analysis was carried out on the samples subjected to the saline crystallization test, after desalination of the fragments by poulticing, and the results are reported in **Figure 7** and **Supplementary Table S2**, in comparison with UT samples (not subjected to any salt crystallization). The differences in the curves for the various treatments and with respect to UT samples are very limited and seem ascribable to the intrinsic variability of the material, which is lower for G and higher for L. In fact, it is noteworthy that, being MIP a destructive test, it was not possible to perform it on exactly the same cylinders before and after the crystallization test. The limited porosity variation is probably related also to the low aggressiveness of the crystallization cycle procedure, which led to a limited deterioration in all the samples.

The results of the tensile splitting test carried out on the stone cylinders after the salt crystallization cycles, drying and brushing, are reported in **Figure 8**. In the case of Globigerina limestone, it can be clearly observed that, for the untreated condition, salt crystallization cycles caused a marked reduction in tensile strength. In the case of the treated specimens, a lower reduction in tensile strength was experienced, the benefit increasing in the order UT ≈ CHIT < HAP < HAP + CHIT. This trend confirms what already found in terms of weight loss (**Figure 5**). In the case of Lecce stone, the results of the tensile splitting test exhibit a less evident trend (**Figure 8A**), but again the HAP + CHIT treatment was able to provide the greatest benefit. In particular, it should be considered that the consolidating treatment of hydroxyapatite increases the strength of the material, which is subsequently decreased by degradation due to salt crystallization test. Therefore, the tensile strength of the L_HAP + CHIT sample, which is higher than the L_UT sample by 9.55%, represents the residual strength after consolidation and subsequent salt degradation. The fact that, for this treatment condition, the residual strength is the highest is in agreement with the lowest weight loss measured at the end of the salt crystallization test for this condition. In fact, the reduced material loss is expected to have helped maintain the high tensile strength even after salt degradation. However, when evaluating the results of the tensile splitting test, it should be kept in mind that only two replicates for each condition were available for each condition, because all the samples were obtained from the same quarry slab (for greater representativeness and homogeneity of the material) and some replicates had been used for other analyses. Additional tests on a higher number of samples will be necessary to confirm the observed trends.

Tests on Prisms

As reported above, the prismatic samples, at the end of the first absorption test, exhibited a considerable amount of efflorescence on the surface, as shown in **Figure 9**, but after brushing no really significant deterioration of the stone substrates was observed. The repetition of the test (on a single sample per type) caused significant degradation, with formation of efflorescence and detachment of a layer from the sample surface, as reported in **Figure 10**. The weight variation of the prisms after the first and the second continuous absorption tests, after drying and brushing ($W_{dry,\ brushed}$), is reported in **Supplementary Figure S2**, while the corresponding changes of final dry weight compared to the initial one (ΔW_{final}), are reported in **Figure 11**. These values refer to the single prismatic sample of each condition that was used for both tests. **Supplementary Table S3** also report a summary of the weight loss reduction caused by the treatments in the two stones in comparison with untreated references, in the two salt crystallization tests. The values in **Figures 9–11** and **Supplementary Table S3** allow to derive some remarks:

FIGURE 9 | Prismatic samples at the end of the first continuous absorption test, before brushing.

- The first absorption test led to an increase in the weight of all samples, due to the accumulation of salt in the stone, but the damage was very limited. The deposition of salts inside both stones was higher for UT samples, indicating that all the treatments favored the formation of efflorescence rather than subflorescence.

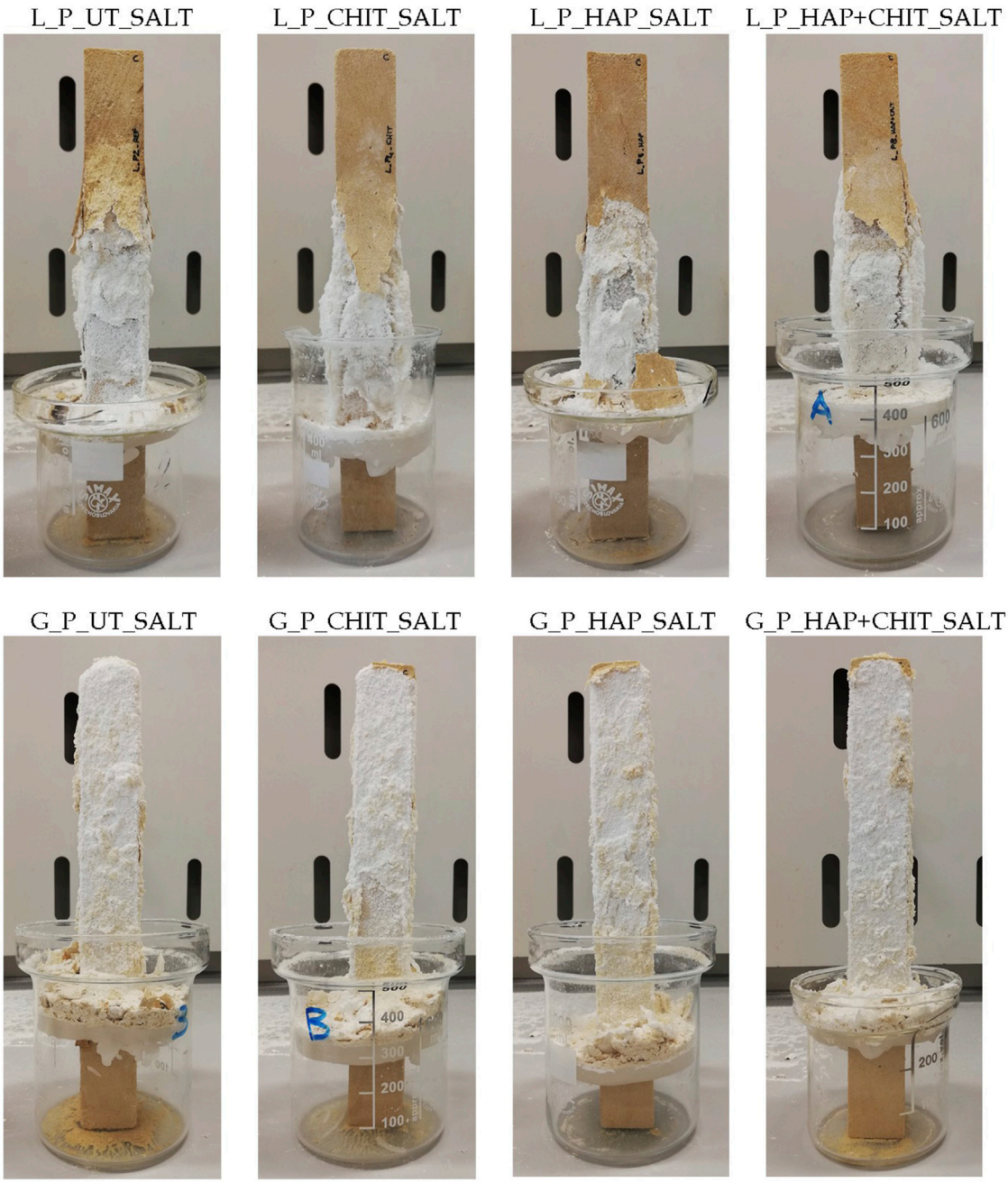

FIGURE 10 | Prismatic samples at the end of the second continuous absorption test, before brushing.

- After the first test, the samples were oven-dried (expectedly causing the formation of thenardite) and the second test started, hence the salt already present in the pores transformed into mirabilite, causing severe deterioration. The final weight loss at the end of the second test was quite limited in L and evident in G. It is interesting to note that the "wick test" carried out on prisms produced a very different damage in the two stones, while their deterioration was similar after the salt crystallization cycles on cylinders (**Figure 5**), although again slightly higher in G than in L. This can be ascribed to the different mechanism of salt damage in the two tests, but also to the smaller thickness of prisms compared to cylinders, making the impact of weight loss larger in the former ones.
- After the second test, all the treatments caused a lower deterioration (smaller weight loss) in the stone samples, the improvement increasing in the following order: CHIT < HAP < HAP + CHIT, again confirming the trend already

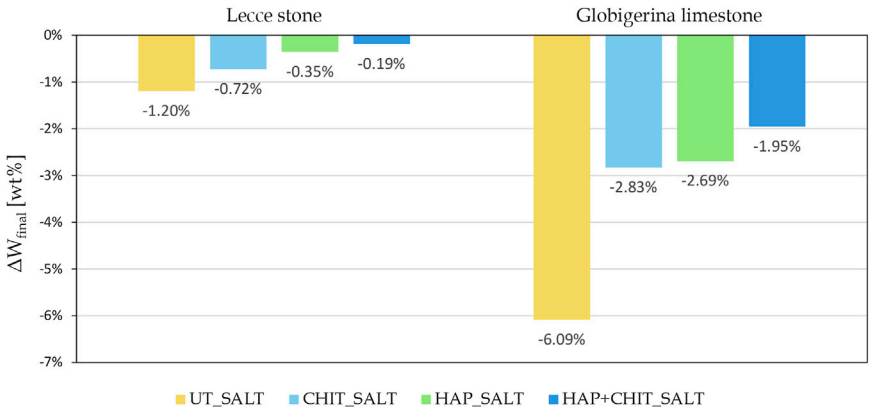

FIGURE 11 | Change in the final dry weight of the prisms after the second absorption test, after brushing, compared to the initial weight for the samples.

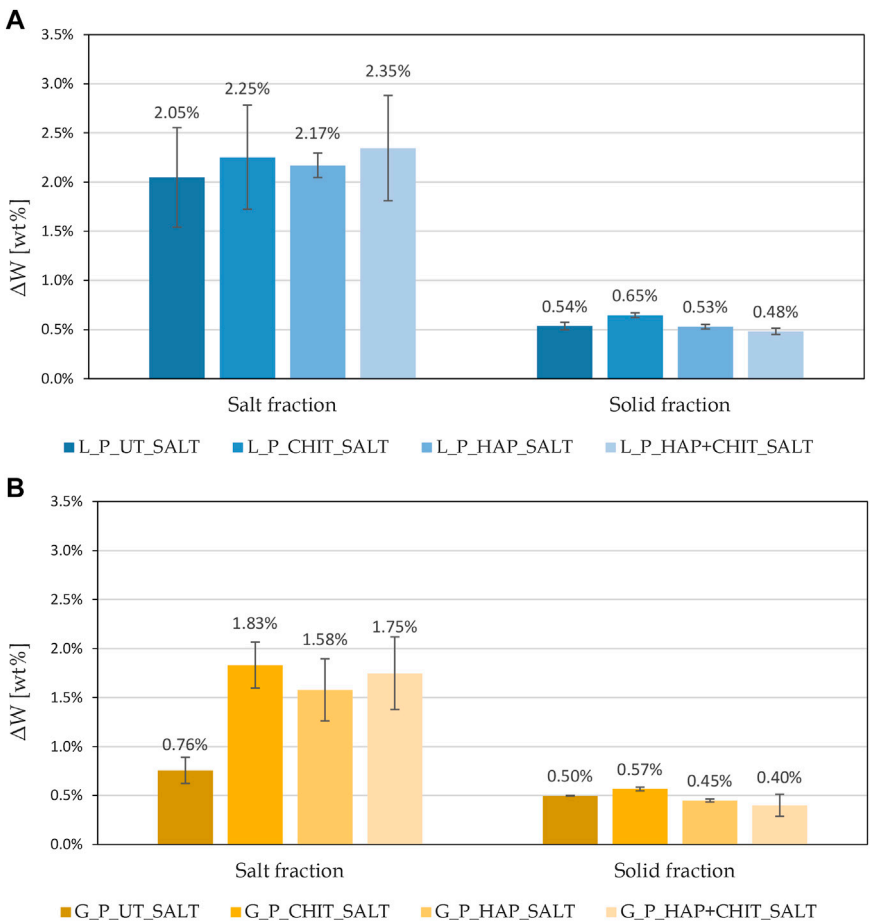

FIGURE 12 | Weight percentages of salt fraction and solid fraction in debris, referred to the initial weight of the prismatic samples, obtained after brushing at the end of the first absorption test, for: **(A)** Lecce stone and **(B)** Globigerina limestone.

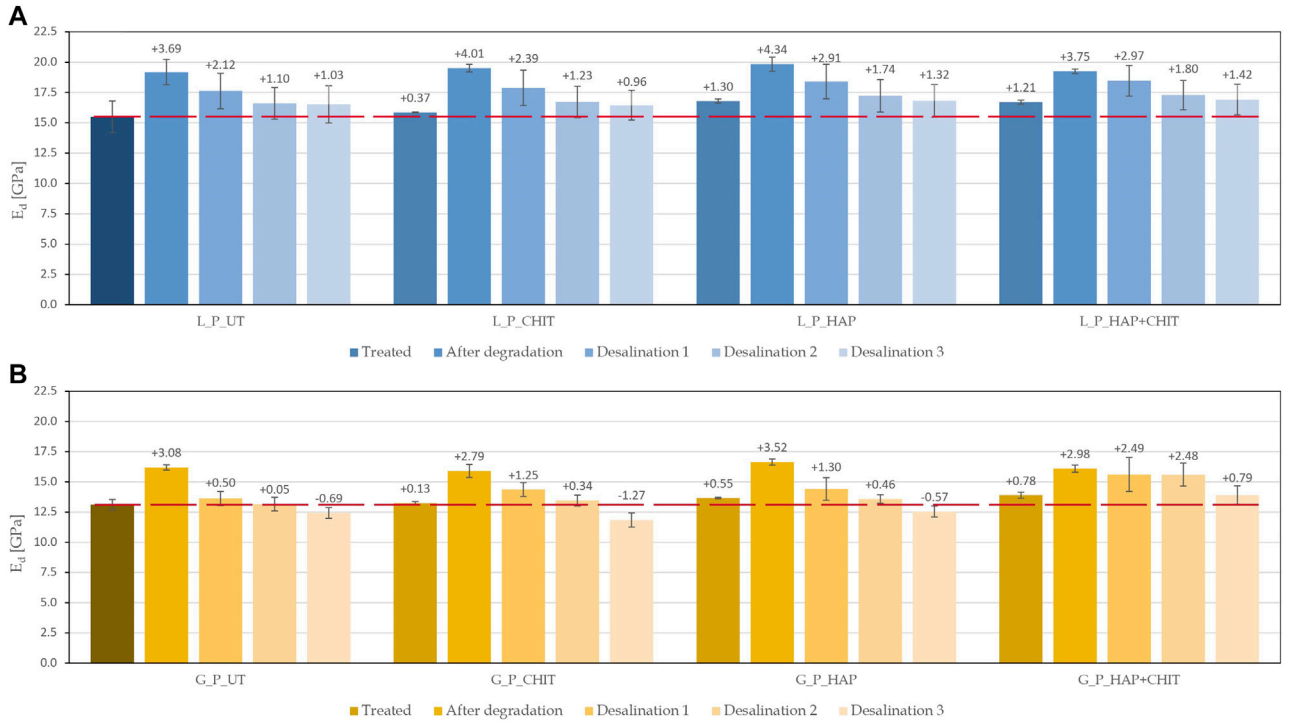

FIGURE 13 | Dynamic elastic modulus of the prismatic samples at each stage of the research (the dotted line indicates the initial value of the UT reference), for: **(A)** Lecce stone and **(B)** Globigerina limestone. The dotted line indicates the initial value of the UT reference (15.49 GPa for L and 13.11 GPa for G).

observed. The combined HAP + CHIT treatment led to a remarkable improvement with respect to the untreated conditions, as the weight loss decreased by 84% in Lecce stone and by 68% in Globigerina limestone, which were actually the same percentages of reduction found in the cylinders. Unlike the crystallization cycles on cylinders, in this case also the chitosan treatment alone led to a significant improvement (**Supplementary Table S3**). This was ascribed to the fact that the chitosan alone was not as well anchored to the pore surface as in the case of the HAP pre-treatment, so it was probably partially removed (alongside calcite) during the multiple wetting cycles carried out in the cylinders, while it was not so altered during the two cycles of continuous absorption carried out in the prisms.

The debris brushed at the end of the first absorption test were analysed and the results are reported in **Figure 12**, as weight percentages of solid fraction (ΔW_{solid}) and sodium sulphate (Na_2SO_4) fraction (ΔW_{salt}) with respect to the initial weight of the samples. The results in terms of stone loss confirm the limited deterioration achieved after the first complete absorption of the saline solution. The presence of chitosan in this type of test, both alone and in combination with hydroxyapatite, caused an increase in the saline fraction, therefore in the amount of efflorescence formed, as can be seen also in **Figure 9**. Moreover, in HAP + CHIT samples, there was also a lower quantity of solid fraction, indicating that the combined treatment has a beneficial effect, promoting efflorescence and limiting damage in the stone. This confirms what was also found in the crystallization test on the cylinders. The CHIT samples, on the other hand, despite a greater quantity of efflorescence than the untreated ones, did not cause any reduction in the solid fraction lost (or even a slight increase), indicating that the polymer alone was not so effective.

Although the weight variation of the samples during the salt crystallization tests can generally provide a useful indication about the deterioration state of the sample, it must be noted that this variation is the sum of a positive term (the salts deposited in the stone pores) and a negative term (the stone debris lost due to deterioration). For this reason, to better evaluate the deterioration of the stone, the dynamic elastic modulus was measured before treatment, after treatment, after the salt crystallization test (after brushing) and also after progressive desalination by poulticing. The values obtained at each phase are reported in **Figure 13**. An increase in the dynamic elastic modulus may indicate an effective consolidation treatment and/or some salt accumulation in the pores, while a reduction indicates internal damage in the material due to salt crystallization (cracking). It is noteworthy that the sensitivity of ultrasonic velocity measurement to micro-cracks development in the stone is very high, as these micro-cracks strongly affect the path followed by ultrasonic wave.

As desirable, after treatments, all the samples showed an increase in the elastic modulus, obviously greater for the

consolidated ones (HAP and HAP + CHIT). After the salt crystallization test, the maximum E_d value was found, as the salt crystals inside the stone samples partially filled the pores and provided a faster ultrasonic transmission. In each of the three desalination phases, the salt ions were transported into the poultice and removed from the samples. Consistently, the elastic modulus progressively decreased after each poultice application, as the pores (previously filled by salts) were progressively emptied. In the case of Globigerina limestone, after desalination for the third time, the UT, CHIT and HAP samples exhibited a lower E_d value than the initial condition, which suggests crack formation during the salt crystallization test. On the contrary, in the case of the HAP + CHIT treatment, the final E_d was still higher than the initial condition (the value being actually very close to that right after treatment), which suggests limited damaging during the salt crystallization test. In the case of Lecce stone, after desalination for 3 times all the specimens exhibited an E_d value still higher than the initial one, again the value of the HAP + CHIT sample being the highest. Although the permanence of some residual salts inside the samples even after the third desalination cannot be completed excluded, still the observed trend confirms the potential of the HAP + CHIT treatment to prevent salt damage.

CONCLUSION

In the present paper, three treatments were tested, aiming at preventing salt crystallization damage in porous limestone: an hydroxyapatite-based consolidant (expected to strengthen the stone), a chitosan solution (expected to inhibit salt crystallization and favor the formation of efflorescence rather than harmful subflorescence) and a combination of these two treatments (where hydroxyapatite is expected to also improve the anchoring of chitosan). Lecce stone and Globigerina limestone were used, being representative of highly porous lithotypes widely used in heritage buildings and severely affected by salt damage onsite.

All the treatments were characterized by low concentration and hence they caused only a slight increase in the weight of the samples, indicating a small amount of products deposited. As a consequence, the treatments basically did not alter the porosity of the stone, demonstrating an excellent compatibility, although they somehow altered the capillary water absorption rate (especially for the combined treatment), although this latter aspect is still under investigation. The possibility that the alteration of the absorption rate given by the treatments is transitory is supported by the results of the crystallization tests. In fact, the prisms, despite absorbing saline solution at slightly different rates, all dried out in similar times (6–7 days); moreover, the weights of the cylinders at the end of the wetting phase of each cycle did not show substantial differences. Therefore, it seems that this slowdown was only transitory and did not have an important impact on the results. This aspect, however, still requires full elucidation and, in order to better understand the transitory or permanent nature of the phenomenon, further tests are necessary. All the treatments also caused a slight increase in the dynamic elastic modulus of the stones, suggesting a positive effect in terms of mechanical properties.

Two accelerated laboratory tests were carried out to investigate the effectiveness of the treatments. The first one was carried out on stone cylinders and involved salt crystallization cycles in a sodium sulphate solution (wetting and drying cycles). These cycles were designed by modifying the procedure of the EN 12370 standard, in order to make the entire test less aggressive than that in the standard. This first kind of salt crystallization test allowed to make the following remarks:

- drying in room conditions (adopted in the first 12 cycles) likely prevented the full transformation thenardite ↔ mirabilite during the cycles, hence it was too mild and made it necessary to adopt oven drying at 50 °C for the following eight cycles. Although a clear weight loss was induced in the samples by this second drying method, an improvement of the procedure used for the cycles still seems necessary, to find a compromise between the too aggressive method suggested by the EN standard and the too mild one adopted in this research;
- all the treatments promoted the formation of efflorescence compared to the untreated stone samples. In the presence of chitosan, this was ascribed to the inhibiting effect of the polymer, while in the case of the HAP treatment alone this seems due to the extremely rough surface of the calcium phosphate phases formed over the pores surface, promoting the water flow towards the stone surface (Scherer and Wheeler, 2008);
- all the treatments led to an improvement in the stone resistance to salt crystallization, measured in terms of sample weight loss. The improvement increased according to the order CHIT < HAP < HAP + CHIT, the combined treatment providing an outstanding improvement (weight loss decrease by 84% in Lecce stone and by 69% in Globigerina limestone, with respect to the untreated samples);
- the combined HAP + CHIT treatment also gave the best results in terms of tensile strength of the stone after the salt crystallization cycles, basically leading to a residual strength after the cycles equal to (or even slightly higher than) the unweathered original stones.

The second test used to investigate the salt crystallization resistance was based on the continuous capillary absorption of a fixed amount of sodium sulphate solution by prismatic stone samples, up to their complete drying ("wick test"). Two complete cycles of absorption were carried out, allowing to derive the following conclusions:

- like in the previous test, all the treatments promoted the formation of efflorescence compared to the untreated stones. This was assessed not only by visual observation, but also by weighing the amount of salts detached/brushed from the samples at the end of the test;
- all the treatments led to an improvement in the stone resistance to salt crystallization. The weight loss decreased according to the same order as in the previous test, the combined treatment providing basically the same outstanding improvement as in the test on cylinders;
- after the test and the desalination of the prismatic samples by poulticing, the dynamic elastic modulus was measured in the

samples. The combined HAP + CHIT treatment confirmed its very good performance, leading to the highest values (even higher than the original unweathered stone samples in the case of Globigerina limestone).

The comparison between the combined HAP + CHIT treatment and other modifiers tested over last years and mentioned in the Introduction is not an easy task, as differences in the materials used or in the test carried out lead to results that are difficult to compare. In (Cassar et al., 2008), prismatic samples of different quality types of Globigerina limestone, untreated and treated with a phosphorylated inhibitor, were subjected to weathering by a sodium sulphate solution, in a test similar to the "wick test" used in this research. The inhibitor led to an improvement in the saline solution capillary flow through the porous materials, helping crystallization occur on the surface of the stone and not within the pores. Moreover, the treatment led to a reduction in debris loss during the salt crystallization test by about 47% with respect to the untreated samples while, in similar conditions, HAP + CHIT reduced the weight loss by 69%. In (Sammut et al., 2014), cubic stone samples of Globigerina limestone, treated with citrate and phosphocitrate with different treatment methods (capillary rise, brushing and poultice), were subjected to salt crystallization cycles. Although the treatment gave positive effects on the rate of transport of the saline solution, data on the stone loss during crystallization cycles are not reported, as the differences obtained in various conditions were too small to draw conclusions. Other examples, were different substrates or types of tests were used, are reported in (Rodriguez-Navarro et al., 2002; Selwitz and Doehne, 2002; Lubelli and van Hees, 2007; Rivas et al., 2010; Ruiz-Agudo et al., 2010; Smith et al., 2010; Gupta et al., 2012; Ruiz-Agudo et al., 2012; Granneman et al., 2019; Bracciale et al., 2020). Concerning the cost of the investigated treatment, the experimental campaign is at an early stage, hence this aspect has not been specifically evaluated yet. However, considering that the most expensive chemical used is chitosan and that its concentration in solution is very low (0.05 wt%), the cost/liter of the chitosan treatment is expected to be comparable with other commonly used conservation treatments. Moreover, chitosan is presently exploited in a wide variety of applications and its use is expected to strongly increase in the future, suggesting that its cost might decrease thanks to the set-up of improved technologies for its production.

The combined treatment, composed by a first application of phosphate consolidant and a second application of a chitosan solution, gave extremely promising results in terms of reduction of salt deterioration in both the porous limestones investigated in this study, with an improvement in the reduction of salt deterioration in line or even greater than other crystallization modifiers. The calcium phosphate phases formed in the first step of the treatment have been shown to improve the tensile strength of stone and to favor the formation of efflorescence rather than subflorescence, but they are also thought to improve the anchoring of the chitosan layer and to prevent the leaching of the calcite substrate, which might lead to the leaching of the chitosan layer too.

The water-based hydroxyapatite consolidant is known to be compatible with stone and friendly for the environment and the conservators, and chitosan is a non-toxic and environmentally friendly biopolymer, hence the combined treatment can be seen as a fully "green" solution for conservation.

The performance of the tested treatments was investigated in this paper through short-term laboratory tests on stone specimens, with encouraging results, but further tests will be necessary to assess the long-term effectiveness and the actual duration of the new treatments. In particular, the fact that chitosan is expected to biodegrade with time is considered a positive feature, which avoids that aged and useless polymeric residues remain in the stone and which can be coped with by periodically re-applying the treatment. However, the duration of this polymer in onsite conditions needs to be investigated, in order to assess whether it is compatible with applications in the conservation field. The effectiveness of the new treatments in different heritage substrates is a further aspect needing investigation and requiring further studies.

DATA AVAILABILITY STATEMENT

The original contributions presented in the study are included in the article/**Supplementary Material**, further inquiries can be directed to the corresponding author.

AUTHOR CONTRIBUTIONS

All authors have read and agree to the published version of the manuscript. Author Contributions: Conceptualization, EF; methodology, EF, ES and MB; experimental investigation: MB and ES; data analysis and interpretation, EF, MB and ES; writing—original draft preparation, MB and EF; writing—review and editing, EF, ES and MB; supervision, EF.

ACKNOWLEDGMENTS

All the members of the RILEM Technical Committee "271-ASC: Accelerated laboratory test for the assessment of the durability of materials with respect to salt crystallization" (Chair: Barbara Lubelli, Deputy Chair: Inge Rörig-Dalgaard) are gratefully acknowledged for the interesting and fruitful discussion about the aggressiveness of standard salt crystallization tests.

SUPPLEMENTARY MATERIAL

The Supplementary Material for this article can be found online at: https://www.frontiersin.org/articles/10.3389/fmats.2021.583112/full#supplementary-material.

REFERENCES

Andreotti, S., Franzoni, E., Degli Esposti, M., and Fabbri, P. (2018). Erratum: Andreotti, S.; Franzoni, E.; fabbri, P. Poly(hydroxyalkanoate)s-Based hydrophobic coatings for the protection of stone in cultural heritage. Materials 2018, 11, 165. *Materials* 11 (3), 389. doi:10.3390/ma11030389

Andreotti, S., Franzoni, E., Ruiz-Agudo, E., Scherer, G. W., Fabbri, P., Sassoni, E., et al. (2019). New polymer-based treatments for the prevention of damage by salt crystallization in stone. *Mater. Struct.* 52 (17), 1–28. doi:10.1617/s11527-018-1309-6

Angeli, M., Jean-Philippe, B., Benavente, D., Menéndez, B., Hébert, R., and David, C. (2007). Salt crystallization in pores: quantification and estimation of damage. *Environ. Geol.* 52 (2), 187–195. doi:10.1007/s00254-006-0474-z

Bracciale, M. P., Sammut, S., Cassar, J., Santarelli, M. L., and Marrocchi, A. (2020). Molecular crystallization inhibitors for salt damage control in porous materials: an overview. *Molecules* 25 (8), 1873. doi:10.3390/molecules25081873

Calia, A., Laurenzi Tabasso, M., Maria Mecchi, A., and Quarta, G. (2013). The study of stone for conservation purposes: Lecce stone (Southern Italy). *Geol. Soci., London, Special Publications* 391 (1), 139–156. doi:10.1144/sp391.8

Cassar, J., Marrocchi, A., Santarelli, M. L., and Muscat, M. (2008). Control de los daños por cristalizaciòn en la caliza de Malta mediante inhibidores de sales. *Materiales de Costrucciòn* 58, 289–290. doi:10.3989/mc.2008.v58.i289-290.83

Charola, A. E., and Bläuer, C. (2015). Salts in masonry: an overview of the problem. *RBM.* 21 (4-6), 119–135. doi:10.1515/rbm-2015-1005

Charola, A. E. (2000). Salts in the deterioration of porous materials: an overview. *J. Am. Inst. Conserv.* 39 (3), 327–343. doi:10.1179/019713600806113176

Charola, A. E., and Wendler, E. (2015). An overview of the water-porous building materials interactions. *RBM.* 21 (2-3), 55–65. doi:10.1515/rbm-2015-2006

Doehne, E., and Price, C. A. (2010). *Stone conservation: an overview of current research*. 2nd Edn, Los Angeles, CA, United States: Getty Publications

EN 12370 (1999). *Natural stone test methods – determination of resistance to salt crystallization*, United Kingdom: BSI

EN 15801 (2009). *Conservation of cultural property – test methods – determination of water absorption by capillarity*, Santry Dublin, Ireland: NSAI

Espinosa-Marzal, R. M., and Scherer, G. W. (2010). Advances in understanding damage by salt crystallization. *Acc. Chem. Res.* 43 (6), 897–905. doi:10.1021/ar9002224

Espinosa-Marzal, R. M., and Scherer, G. W. (2009). Crystallization of sodium sulfate salts in limestone. *Environ. Earth Sci.* 56, 605–621. doi:10.1007/s00254-008-1441-7

Flatt, R. J., Caruso, F., Sanchez, A. M., and Scherer, G. W. (2014). Chemo-mechanics of salt damage in stone. *Nat. Commun.* 5, 4823. doi:10.1038/ncomms5823

Flatt, R. J. (2002). Salt damage in porous materials: how high supersaturations are generated. *J. Cryst. Growth* 242 (3-4), 435–454. doi:10.1016/s0022-0248(02)01429-x

Franceschini, M., Broggi, A., Bracciale, M. P., Sommei, L., Santarelli, M. L., and Marrocchi, A. (2015). Effectiveness of phosphocitrate as salt crystallization inhibitor in porous materials: case study of the roman mosaic ofOrpheus and the beasts(Perugia, Italy). *Int. J. Architect. Herit.* 9 (3), 195–200. doi:10.1080/15583058.2012.760121

Franzoni, E. (2014). Rising damp removal from historical masonries: a still open challenge. *Construct. Build. Mater.* 54, 123–136. doi:10.1016/j.conbuildmat.2013.12.054

Franzoni, E., Sassoni, E., and Graziani, G. (2015). Brushing, poultice or immersion? The role of the application technique on the performance of a novel hydroxyapatite-based consolidating treatment for limestone. *J. Cult. Herit.* 16 (2), 173–184. doi:10.1016/j.culher.2014.05.009

Franzoni, E. (2018). State-of-the-art on methods for reducing rising damp in masonry. *J. Cult. Herit.* 31, S3–S9. doi:10.1016/j.culher.2018.04.001

Goudie, A. S. (1986). Laboratory simulation of "the wick effect" in salt weathering of rock. *Earth Surf. Process. Landforms* 11 (3), 275–285. doi:10.1002/esp.3290110305

Granneman, S. J. C., Lubelli, B., and van Hees, R. P. J. (2019). Mitigating salt damage in building materials by the use of crystallization modifiers—a review and outlook. *J. Cult. Herit.* 40, 183–194. doi:10.1016/j.culher.2019.05.004

Granneman, S. J. C., Shahidzadeh, N., Lubelli, B., and van Hees, R. P. J. (2017). Effect of borax on the wetting properties and crystallization behavior of sodium sulfate. *CrystEngComm* 19 (7), 1106–1114. doi:10.1039/c6ce02163h

Graziani, G., Sassoni, E., and Franzoni, E. (2015). Consolidation of porous carbonate stones by an innovative phosphate treatment: mechanical strengthening and physical-microstructure compatibility in comparison with TEOS-based treatments. *Heritage Science* 3 (1), 1–6. doi:10.1186/s40494-014-0031-0

Graziani, G., Sassoni, E., Franzoni, E., and Scherer, G. W. (2016). Hydroxyapatite coatings for marble protection: optimization of calcite covering and acid resistance. *Appl. Surf. Sci.* 368, 241–257. doi:10.1016/j.apsusc.2016.01.202

Gupta, S., Terheiden, K., Pel, L., and Sawdy, A. (2012). Influence of ferrocyanide inhibitors on the transport and crystallization processes of sodium chloride in porous building materials. *Cryst. Growth Des.* 12 (8), 3888–3898. doi:10.1021/cg3002288

Houck, J., and Scherer, G. W. (2006). Controlling stress from salt crystallization. *Fracture and failure of natural building stones*. Dordrecht, The Nederlands: Springer, 299–312. Chap 5

Lubelli, B., Cnudde, V., Diaz-Goncalves, T., Franzoni, E., van Hees, R. P. J., Ioannou, I., et al. (2018). Towards a more effective and reliable salt crystallization test for porous building materials: state of the art. *Mater. Struct.* 51 (2), 1–21. doi:10.1617/s11527-018-1180-5

Lubelli, B., and van Hees, R. P. J. (2007). Effectiveness of crystallization inhibitors in preventing salt damage in building materials. *J. Cult. Herit.* 8 (3), 223–234. doi:10.1016/j.culher.2007.06.001

Muxika, A., Etxabide, A., Uranga, J., Guerrero, P., and de la Caba, K. (2017). Chitosan as a bioactive polymer: processing, properties and applications. *Int. J. Biol. Macromol.* 105 (2), 1358–1368. doi:10.1016/j.ijbiomac.2017.07.087

Naidu, S., and Scherer, G. W. (2014). Nucleation, growth and evolution of calcium phosphate films on calcite. *J. Colloid Interface Sci.* 435, 128–137. doi:10.1016/j.jcis.2014.08.018

Naidu, S., Sassoni, E., and Scherer, G. W. (2011). New treatment for corrosion-resistant coatings for marble and consolidation of limestone. in Jardins de Pierres – Conservation of stone in Parks, Gardens and Cemeteries, Paris, France, June 2011, 289–294

Ocak, Y., Sofuoglu, A., Tihminlioglu, F., and Böke, H. (2009). Protection of marble surfaces by using biodegradable polymers as coating agent. *Prog. Org. Coating* 66 (3), 213–220. doi:10.1016/j.porgcoat.2009.07.007

Ocak, Y., Sofuoglu, A., Tihminlioglu, F., and Böke, H. (2015). Sustainable bio-nano composite coatings for the protection of marble surfaces. *J. Cult. Herit.* 16 (3), 299–306. doi:10.1016/j.culher.2014.07.004

Pedna, A., Pinho, L., Frediani, P., and Mosquera, M. J. (2016). Obtaining SiO 2 -fluorinated PLA bionanocomposites with application as reversible and highly-hydrophobic coatings of buildings. *Prog. Org. Coating* 90, 91–100. doi:10.1016/j.porgcoat.2015.09.024

Philibert, T., Lee, B. H., and Fabien, N. (2017). Current status and new perspectives on chitin and chitosan as functional biopolymers. *Appl. Biochem. Biotechnol.* 181 (4), 1314–1337. doi:10.1007/s12010-016-2286-2

Rivas, T., Alvarez, E., Mosquera, M. J., Alejano, L., and Taboada, J. (2010). Crystallization modifiers applied in granite desalination: the role of the stone pore structure. *Construct. Build. Mater.* 24 (5), 766–776. doi:10.1016/j.conbuildmat.2009.10.031

Rodriguez-Navarro, C., Doehne, E., and Sebastian, E. (2000). How does sodium sulfate crystallize? Implications for the decay and testing of building materials. *Cement Concr. Res.* 30 (10), 1527–1534. doi:10.1016/s0008-8846(00)00381-1

Rodriguez-Navarro, C., Linares-Fernandez, L., Doehne, E., and Sebastian, E. (2002). Effects of ferrocyanide ions on NaCl crystallization in porous stone. *J. Cryst. Growth* 243 (3-4), 503–516. doi:10.1016/s0022-0248(02)01499-9

Ruiz-Agudo, E., Lubelli, B., Sawdy, A., van Hees, R., Price, C., and Rodriguez-Navarro, C. (2010). An integrated methodology for salt damage assessment and remediation: the case of San Jerónimo Monastery (Granada, Spain). *Environ Earth Sci* 63 (7), 1475–1486. doi:10.1007/s12665-010-0661-9

Ruiz-Agudo, E., Putnis, C. V., Pel, L., and Rodriguez-Navarro, C. (2012). Template-assisted crystallization of sulfates onto calcite: implications for the prevention of salt damage. *Cryst. Growth Des.* 13 (1), 40–51. doi:10.1021/cg300744x

Ruiz-Agudo, E., Rodriguez-Navarro, C., and Sebastián-Pardo, E. (2006). Sodium sulfate crystallization in the presence of phosphonates: implications in ornamental stone conservation. *Cryst. Growth Des.* 6 (7), 1575–1583. doi:10.1021/cg050503m

Sammut, S., Cassar, J., Marrocchi, A., Santarelli, M. L., Russo, C., and Sommei, L. (2014). Investigating a method to limit damage in Globigerina limestone, a soft porous stone widely used in historic buildings. Proceedings of SWBSS 2014 3rd international conference on salt weathering of buildings and stone sculptures, Brussels, Belgium, 14-16 October 2014. Royal Institute for Cultural Heritage Brussels, 101–115

Sandrolini, F., and Franzoni, E. (2007). Repair Systems for the Restoration of Ancient Buildings—dampness Rise Problem/Instandsetzungssysteme für das Restaurieren historischer Gebäude—aufsteigende feuchtigkeit. *RBM.* 13 (3), 161–172. doi:10.1515/rbm-2007-6129

Sassoni, E., Franzoni, E., Stefanova, M., Kamenarov, Z., Scopece, P., and Verga Falzacappa, E. (2020). Comparative study between ammonium phosphate and ethyl silicate towards conservation of prehistoric paintings in the magura cave (Bulgaria). *Coatings* 10 (3), 250. doi:10.3390/coatings10030250

Sassoni, E., Graziani, G., and Franzoni, E. (2016a). An innovative phosphate-based consolidant for limestone. Part 1: effectiveness and compatibility in comparison with ethyl silicate. *Construct. Build. Mater.* 102 (1), 918–930. doi:10.1016/j.conbuildmat.2015.04.026

Sassoni, E., Graziani, G., and Franzoni, E. (2016b). An innovative phosphate-based consolidant for limestone. Part 2: durability in comparison with ethyl silicate. *Construct. Build. Mater.* 102 (1), 931–942. doi:10.1016/j.conbuildmat.2015.10.202

Sassoni, E., Graziani, G., Franzoni, E., and Scherer, G. W. (2018). Calcium phosphate coatings for marble conservation: influence of ethanol and isopropanol addition to the precipitation medium on the coating microstructure and performance. *Corrosion Sci.* 136, 255–267. doi:10.1016/j.corsci.2018.03.019

Sassoni, E. (2018). Hydroxyapatite and other calcium phosphates for the conservation of cultural heritage: a review. *Materials* 11 (4), 1–48. doi:10.3390/ma11040557

Sassoni, E., Naidu, S., and Scherer, G. W. (2011). The use of hydroxyapatite as a new inorganic consolidant for damaged carbonate stones. *J. Cult. Herit.* 12 (4), 346–355. doi:10.1016/j.culher.2011.02.005

Scherer, G. W. (1999). Crystallization in pores. *Cement Concr. Res.* 29 (8), 1347–1358. doi:10.1016/s0008-8846(99)00002-2

Scherer, G. W. (2004). Stress from crystallization of salt. *Cement Concr. Res.* 34 (9), 1613–1624. doi:10.1016/j.cemconres.2003.12.034

Scherer, G. W., and Wheeler, G. S. (2008). Silicate consolidants for stone. *Kemi* 391, 1–25. doi:10.4028/www.scientific.net/kem.391.1

Selwitz, C., and Doehne, E. (2002). The evaluation of crystallization modifiers for controlling salt damage to limestone. *J. Cult. Herit.* 3 (3), 205–216. doi:10.1016/s1296-2074(02)01182-2

Smith, B. J., Gomez-Heras, M., Viles, A., and Cassar, J. (2010). *Limestone in the built environment: present-day challenges for the preservation of the past*. London, United Kingdom: Geological Society of London, 331

Steiger, M., and Asmussen, S. (2008). Crystallization of sodium sulfate phases in porous materials: the phase diagram Na2SO4-H2O and the generation of stress. *Geochem. Cosmochim. Acta* 72 (17), 4291–4306. doi:10.1016/j.gca.2008.05.053

Tsui, N., Flatt, R. J., and Scherer, G. W. (2003). Crystallization damage by sodium sulfate. *J. Cult. Herit.* 4 (2), 109–115. doi:10.1016/s1296-2074(03)00022-0

Conflict of Interest: The authors declare that the research was conducted in the absence of any commercial or financial relationships that could be construed as a potential conflict of interest.